Cross-Shelf transport by (storm-modified, sandy) hyperpycnal flows in the Eastern Rhenish Massif during the Upper Eifelian, Middle Devonian

Authors: Robin Schaumann (robin.schaumann@outlook.de) and Tom McCann. Both authors are affiliated with the University of Bonn

This paper is a non-peer reviewed preprint submitted to EarthArXiv.

It has been submitted to Sedimentologika and is in review.

Cross-Shelf transport by (storm-modified, sandy) hyperpycnal flows in the Eastern Rhenish Massif during the Upper Eifelian, Middle Devonian

Robin M. Schaumann[1], Tom McCann[1]

[1]Institut für Geowissenschaften, Universität Bonn

Author Note
Robin Schaumann, https://orcid.org/0000-0002-9036-0557
Tom McCann

Correspondence concerning this article should be addressed to: Robin M. Schaumann

Institut für Geowissenschaften
Robin Schaumann
Kirschallee 3
53115 Bonn

Email: robin.schaumann@outlook.de

Abstract

High-resolution sedimentary facies analysis on ten profiles (252.24 m total length) reconstructed a complex depositional system characterised by cross-shelf sediment transport via (storm-modified) hyperpycnal flows in the Unnenberg Formation (Upper Eifelian, Middle Devonian) of the Eastern Rhenish Massif. The hyperpycnal-fed prodeltaic shelf system comprised proximal and distal lobe deposits (=hyperpycnal subaqueous delta) as well as deltaic mid-ramp deposits (=hyperpycnal littoral delta). Facies associations indicated that the hyperpycnal flows were fluctuation, resulting in the development of cyclic sequences of massive, laminated, and rippled sandstones. Plant-rich intervals provide a clear link to terrestrial sources. Hummocky cross-stratification, quasi planar-lamination and combined-flow ripples, suggest combined flow influences, driven by monsoonal dynamics. The presence of elementary depositional sequences (1.5–11 m thick) indicate progradational trends related to climate-driven hyperpycnal processes. Sedimentation rates of 0.15–1.12 m/kyr align with a monsoon-regulated half-precession cycle of 9.8 kyr, suggesting a direct link between climatic forcing and sediment delivery. This research supports the role of hyperpycnal flows in transferring sandy sediments across continental shelves, reinforcing their importance in constructing clastic deltaic ramps and shelfal lobes during the Middle Devonian. The findings contribute to our understanding of sedimentary dynamics in ancient marine systems and highlight the importance of hyperpycnal flows as a key mechanism in sediment distribution from deltaic to deep-marine environments.

Lay Summary

Millions of years ago, powerful underwater currents transported sand and mud from ancient rivers into the ocean, shaping the seafloor. This study examines these currents, known as hyperpycnal flows, which played a crucial role in sediment transport during the Middle Devonian period (about 390 million years ago) in what is now Germany's Rhenish Massif. By careful analysing the Unnenberg Formation, researchers identified different types of sandstone and mudstone deposits that reveal how these flows moved sediments across the continental shelf. The study shows that these flows were influenced by monsoonal climate cycles, which affected the volume and strength of river discharge into the ocean. The findings suggest that hyperpycnal flows helped build deltaic and deep-sea deposits. This improves our understanding of how sediments travel from land to deep marine environments, which is important for studying Earth's history, natural resource distribution, and modern sedimentary processes. By linking climate cycles with sediment transport, this research highlights the impact of long-term climate patterns on marine geology—insights that are also relevant for understanding today's changing environments.

Keywords: Bergisches Land, Unnenberg Formation, combined flow, hummocky cross stratification, elementary depositional sequences

1. Introduction

The Eifelian strata of the Bergisches Land and Sauerland are dominated by clastic marine sediments, with ~3000 m thick sandstones, siltstones and claystones which accumulated in a shelf environment (i.e., the Rhenish shelf) at water depths of 25-300 m (Ribbert & Baumgarten, 2012). Throughout the

Mid-Devonian, transgressive-regressive cycles led to cyclic shifting of the coastline (Langenstrassen, 1983; Reuter, 1993), with the coeval development of extensive deltaic systems distributing large volumes of sediments from Laurussia (=Old Red Continent) onto the Rhenish shelf (Fig. 1; Langenstrassen et al., 1979; Langenstrassen, 1982; Engel et al., 1983; Langenstrassen, 1983; Reuter, 1993; Ribbert & Baumgarten, 2012; Ribbert et al., 2017).

Three phases of pronounced sand deposition are described for the Mid-Devonian in this region. During these phases, closely linked delta-shelf-basin depositional systems developed. These periods of cross-shelf transportation coincided with Mid-Devonian regressional phases (Fig. 2). One well-documented (Pfeiffer, 1938; Thienhaus, 1940; Ribbert & Baumgarten, 2012; Ribbert, 2013; Ribbert et al., 2017) but poorly understood system is the (herein termed) Brandenberg-Unnenberg system, which developed in the Upper Eifelian. This system can be subdivided into distinctive facies realms (i.e., inner shelf, outer shelf, shelf slope, basin). The NW of the system is characterised by deltaic deposits (siltstones, sandstones; Brandenberg Formation) with abundant red beds and conglomerates with an average sedimentation rate of 0.3 m/kyr (Langenstrassen et al., 1979; Reuter, 1993). These inner-shelf deltaic deposits can be correlated with outer shelf sandstones (Unnenberg Formation) which are herein interpreted as having been deposited from putative, sustained (or combined) hyperpycnal flows, which accumulated as shelf lobes. Adjacent shelf slope deposits comprise banded mudstones, with abundant (turbiditic) sandstones (Lennehelle Formation), while basin deposits are dominated by mudstones with rarer intercalated (turbiditic) sandstones (Ramsbeck Formation, Asten Formation, Raumland Formation, Eifel Quarzit). Common to all of the aforementioned deposits are accumulations of land-derived plant fossils and detritus (Ebert & Müller, 1973; Mustafa, 1975; Clausen, 1978; Mustafa, 1978a, 1978b; Langenstrassen et al., 1979; Ribbert, 2013).

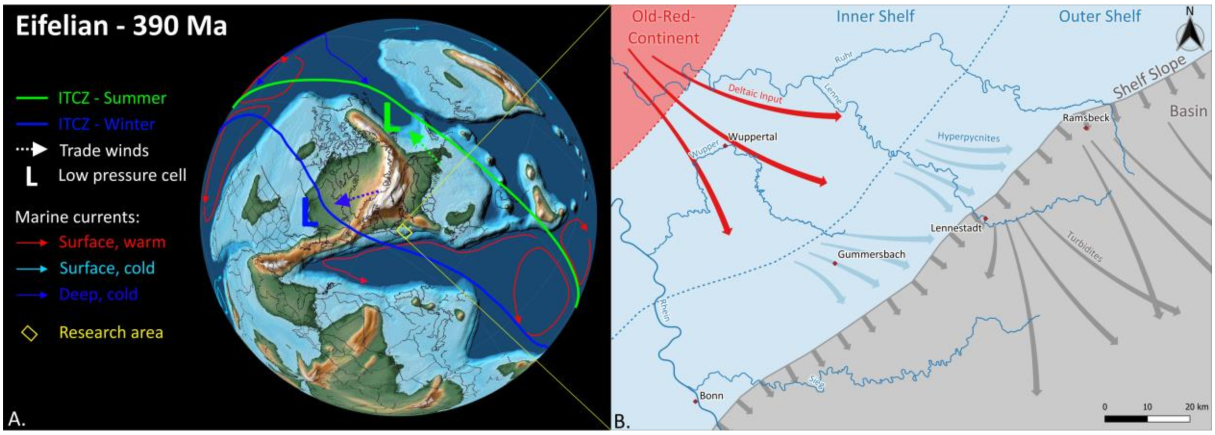

Fig 1: A: Palaeogeography of the Eifelian (Scotese, 2016). Intertropical Convergence Zone (ITCZ), trade winds and low pressure cells (L) after de Vleeschouwer et al. (2012); marine currents after Suttner et al. (2021). B: Palaeogeographical map of the Eifelian of the Bergisches Land, compiled from Meischner (1971) and Ribbert et al. (2017).

The recognition of hyperpycnal flows as a distinctive form of sediment-laden turbulent flow in areas transitional from river deltas to the shallow ocean was initially developed by Mulder et al. (2003). These authors suggested that a hyperpycnal flow forms due to the direct discharge of sediment-water mixtures by river floods, and that the subsequent deposits can be classified as hyperpycnites (Mulder et al. 2003). Despite some discussion (Shanmugam, 2018, 2019; van Loon et al., 2019; Zavala, 2019), hyperpycnal flows are broadly recognised as a major pathway of transferring material across the shelf into the deeper parts of a marine depositional basin (Steel et al., 2018; Heerema et al., 2020; Zavala, 2020; Rodríguez-Tovar, 2022; Beelen & Wood, 2023; Grundvåg et al., 2023; Luo et al., 2023). A hyperpycnal flow develops as a result of the discharge of riverine waters with a high suspended load (i.e., bulk density of 35-45 kg/m^3) into a body of water. When the bulk density of the incoming river flow exceeds that of the receiving water body, the fluvial discharge sinks and forms a hyperpycnal flow at the bottom of the water body. This also results in a downwelling of surface waters, forcing less dense extrabasinal material, such as plant debris (e.g. leaves, branches, twigs, trunks) and charcoal (and possibly algal material) to sink and to be transported along with the hyperpycnal discharge (Mulder et al., 2003; Zavala & Arcuri, 2016; Zavala & Pan, 2018). Such flows can travel long distances across the shelf area (Mulder et al., 2003; Steel et al., 2016; Zavala & Arcuri, 2016; Zavala & Pan, 2018) and flow times can last from weeks to months (Zavala & Pan, 2018). In contrast to intrabasinal (classical) turbidites (average velocity up to 7.2 m/s, Heerema et al., 2020), hyperpycnal flows are slow-moving (average velocity 0.2 m/s at the leading head, Zavala & Pan, 2018) dynamic jet flows (Hoyal et al., 2003). Day- to month-long pulsing of rivers in flood (i.e., long-lived hyperpycnal flows) will generate a complex stacking of beds and bedsets (Zavala & Pan, 2018; Zavala, 2020). According to Zavala et al. (2011a), deposits of sustained hyperpycnal flows can be attributed to three main genetic facies groups, which broadly correspond to bed load, suspended load, and lofting transport processes, and thus represent a proximal-distal distribution within the depositional setting.

Aims: This study suggests that a hyperpycnal, shuttling process transported fine-grained material from a deltaic coast, across the outer shelf, and into the neritic basin. This process is well-documented by the deposits of the Unnenberg Formation near Gummersbach in the Bergisches Land. Based on high-resolution sedimentary facies analysis, the dominant depositional processes of the Unnenberg Formation will be elaborated and compared to hyperpycnal systems in order to precisely determine the depositional environment, and how it changed over time.

2. Geological Setting

Sedimentation throughout the Devonian occurred in a marine basin located close to the equator (Ribbert & Baumgarten, 2012; Ribbert et al., 2017; Franke, 2024). The basin was bounded to the N by Laurussia and to the S by the Mid-German High (Stets & Schäfer, 2002). This marine basin is commonly referred to as the Rhenish Trough, and is a peripheral basin of the narrow (about 250-530 km) but elongate (more than 2000 km) Rhenohercynian Basin. In this context, the Rhenohercynian Basin is considered to be a marginal basin of the Rheic Ocean (Stets & Schäfer, 2002; Königshof et al., 2016; Franke, 2024). Laurussia served primarily as a source area, providing several thousand metres of eroded sediment which resulted in significant sediment loading (possibly accentuated by external forces), and resultant crustal subduction in the area of the Rhenish Trough (Ribbert et al., 2017).

2.1 Unnenberg Formation

Locus typicus: N 51.055754 E 7.617517 (Fuchs, 1919)

The Unnenberg Formation (Fig. 2-3) comprises thin- to thick-bedded, mica-rich, fine-grained sandstones (Fuchs, 1922, 1923; Fuchs & Schmidt, 1928; Dietz & Fuchs, 1935; Grabert, 1969, 1970; Ziegler, 1970; Grabert, 1971; Ziegler, 1978; Jux, 1983; Ribbert, 2013). The sandstones are blueish-grey, though they weather to a reddish-brown. The sandstones are commonly intercalated with dark-blueish siltstones and blackish-grey silty to sandy mudstones. Fuchs and Schmidt (1928) noted that these siltstones and mudstones tend to dominate the Unnenberg Formation in the central Sauerland region. Thienhaus (1940) described lithofacies variations in the Attendorner syncline area (i.e. central Sauerland) where fine-grained sandstones, organic-rich sandy mudstones with intercalated sandstones, and banded mudstones with intercalated carboniferous quartzites tend to predominate. A range of sedimentary structures are described for the Unnenberg Formation, including cross-bedding, planar-lamination, fining upwards sequences, and internal slumping, as well as ripple marks on bed tops and groove marks at bed bases. Furthermore, plant remains and bioclastic lags are abundant. Some beds are completely bioturbated (Fuchs, 1922, 1923; Fuchs & Schmidt, 1928; Dietz & Fuchs, 1935; Grabert, 1969, 1970; Ziegler, 1970; Grabert, 1971; Ziegler, 1978; Jux, 1983; Ribbert, 2013). Fossil lists of the Unnenberg Formation have been published by Thienhaus (1940) and Spriestersbach (1942).

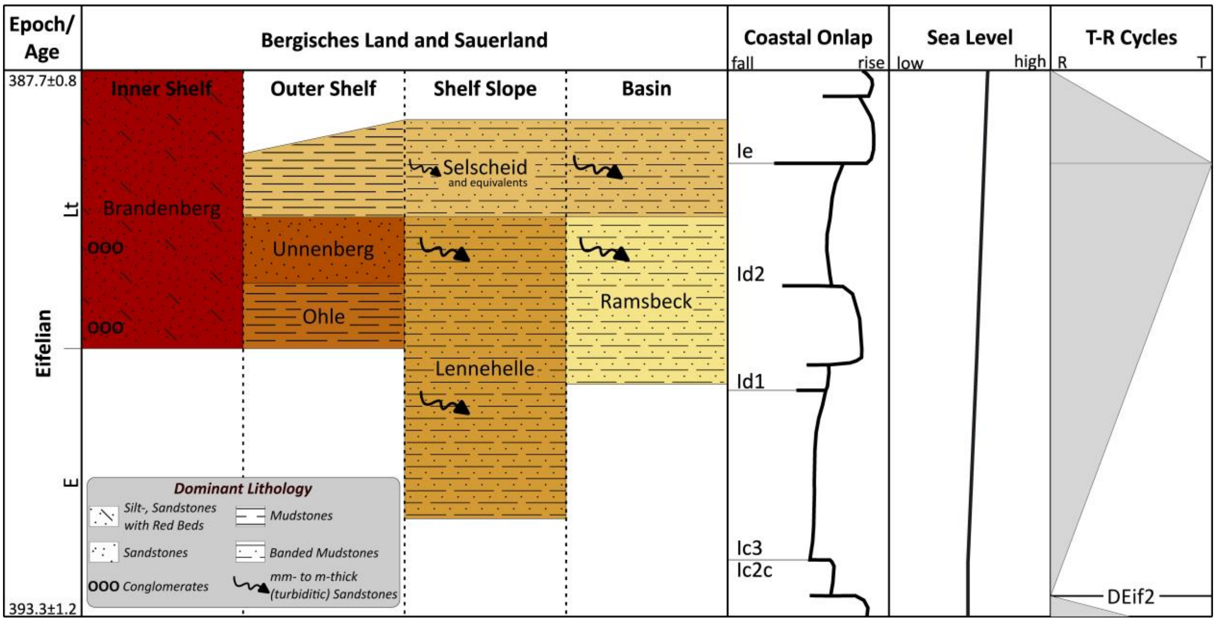

Fig 2: Stratigraphic table of the Bergisches Land and Sauerland during the Eifelian. Stratigraphy after Ribbert (1998a; 1998b, 1998c, 1998d, 1998e, 1998f, 1998g, 1998h, 1998i, 1998j, 1998k). Coastal onlap after Johnson et al. (1985), redrawn from Becker et al. (2020). Sea level and T-R cycles redrawn from Becker at al. (2020).

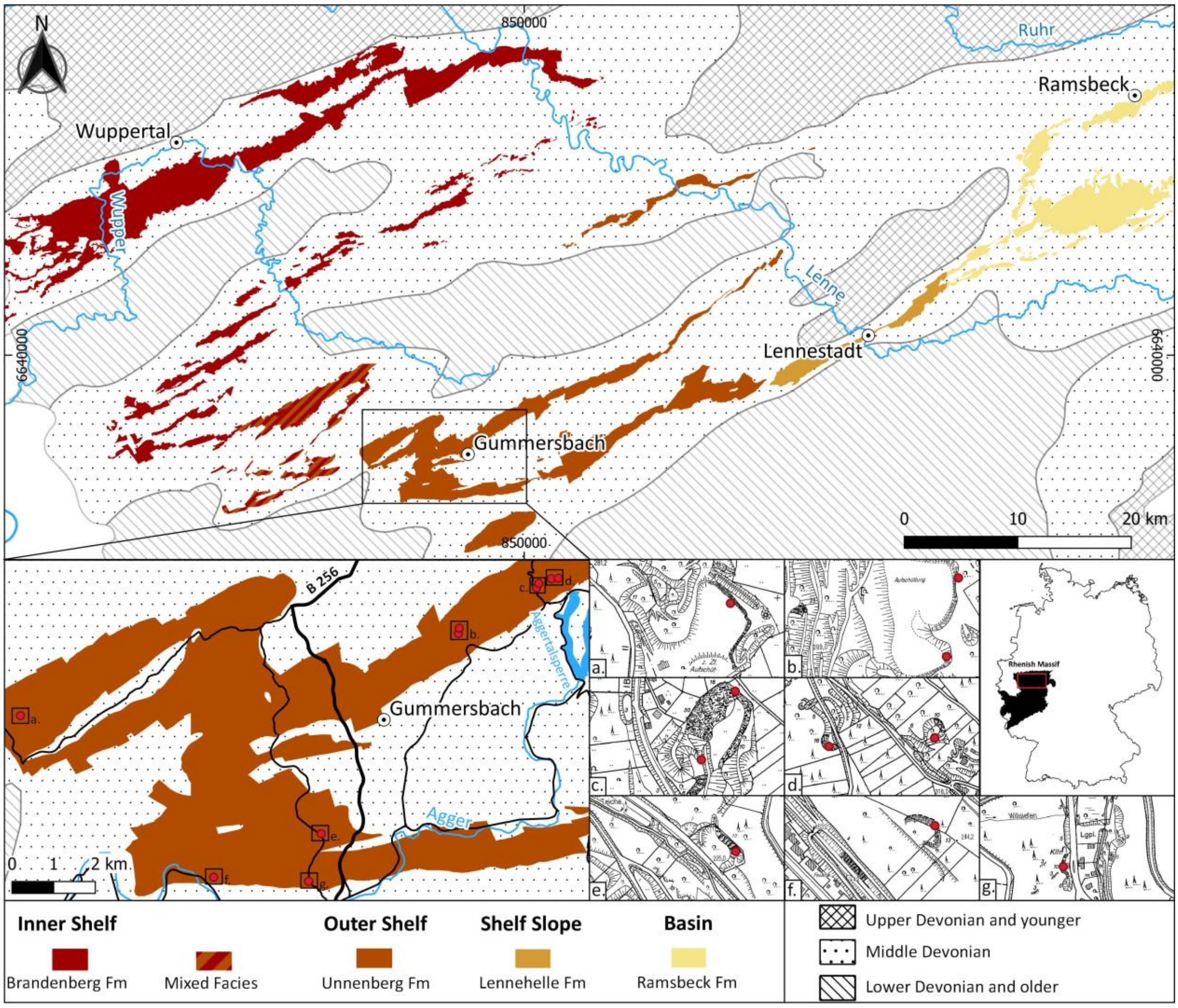

Fig 3: Geological map of the Bergisches Land and the Sauerland. Outcrops/Profiles (Fig. 9-10) are a. Hagen 2; b. Talbecke Ost 2, Talbecke Ost 2 Nebenbruch; c. Unnenberg lower level, Unnenberg upper level; d. Ratemicke West, Ratemicke Ost; e. Oesinghausen; f. Liefenroth; g. Vollmershausen.

3. Methods

To determine the depositional processes, which led to the deposition of the Unnenberg Formation near Gummersbach, ten sedimentary profiles with a total length of 252.24 m were measured during a field campaign extending from March to September of 2021. Outcrops were selected following a GIS-based analysis of the study area, together with field observations.

The sedimentary facies analysis which was carried out on the sediments of the Unnenberg Formation was informed by the genetic facies tracts of sustained hyperpycnal flows of Zavala *et al.* (2011). Thus, each of the recognised sedimentary facies were described in terms of their sediment characterisation (e.g. sediment grain size, sorting), sedimentary structures (e.g. lamination, evidence of reworking, bioturbation), macrofaunal characterisation, the presence and nature of organic matter (e.g. plant remains), and the presence of sharp, erosional or gradual contacts. The sediments were also tested with dilute hydrochloric acid (10%) for carbonates.

4. Results

Petrographic analysis of the Unnenberg Formation sediments reveals that they are submature to mature and moderately to well-sorted. Individual grains are angular to subangular (some rounded grains were noted as well), with a low to moderate sphericity. Grain contacts tend to be long or concave-convex, and rarely sutured. A Q-F-L sandstone classification of the sandstones after Folk (1974) shows that the samples plot mainly within the sublitharenite field, with one specimen plotting within the subarkose field (Fig. 4). In addition to quartz, rare feldspars (plagioclase > K-feldspar), muscovite, biotite, chlorite, and rare zircon, rutile and garnet were noted.

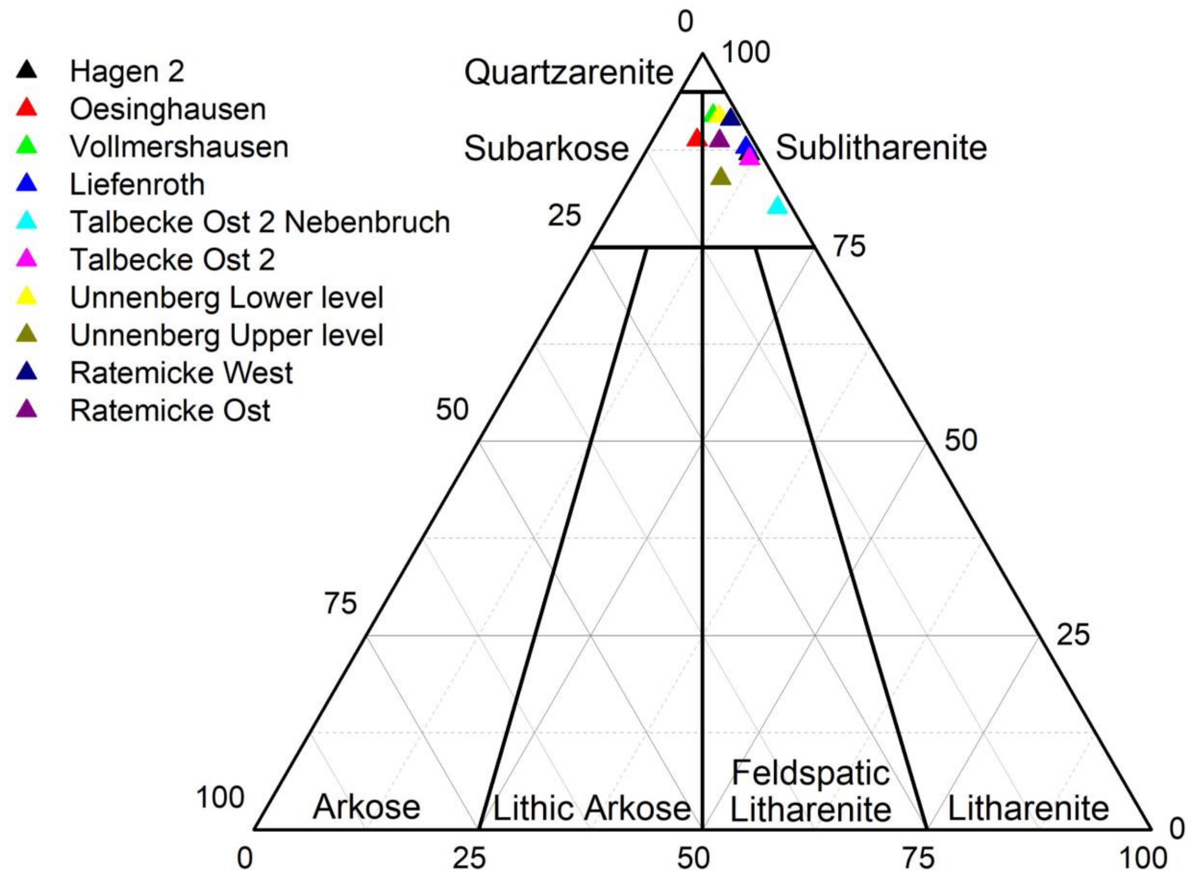

Fig 4: Sandstone classification after Folk (1974). The sample from the Oesinghausen profile plots within the Subarkose field. The remaining samples plot within the Sublitharenite field.

Tab 1: Facies description and interpretation of depositional origin:

Facies		Thickness [cm]	Lithology	Sedimentary structures	Bioturbation	Interpretation	Facies Zavala	Facies association
F1	F1a	5-300	Fine-grained sandstones	Massive	Branched and wielding, horizontal burrows	Suspended Load, progressive aggradation by sustained hyperpycnal flows	S1	Sandy hyperpycnal flow
	F1b	32-250	Fine-grained sandstones, abundant crinoid columnals	Massive	Horizontal burrows	As above; crinoid entrainment; dragging and rolling of crinoid columnals at the base of the suspension cloud		
F2	F2a	5.5-220	Fine-grained sandstones	Planar-lamination, ball structures	Straight, horizontal burrows; system of wielded and branched, horizontal burrows	Suspended Load, gravitational collapse of sustained hyperpycnal flows	S2	
	F2b	17-749	Fine-grained sandstones, abundant crinoid columnals	Planar-lamination	-	As above; crinoid entrainment; dragging and rolling of crinoid columnals at the base of the suspension cloud		
F3		101	Fine-grained sandstones	Climbing ripples	-	Suspended Load, traction plus fallout by overpassing and wanning hyperpycnal flow	S3	
F4		3-50	Siltstones and mudstones	Massive, planar lamination	(Cross-cutting), horizontal burrows, complete bioturbation of beds	Suspended load, fallout from stationary suspension cloud, which is produced from the dying turbidity current (hemiturbidite)	S4	

F5		10-60	Fine-grained sandstones, siltstones, plant debris	Planar-lamination	Branched, horizontal burrows	Lofting, fallout from lofting plumes	L	
F6		16-25	Fine-grained sandstones, siltstone-levels, plant debris	Planar-lamination	-	Suspended Load/lofting, gravitational collapse of sustained hyperpycnal flows at the channel margin or levee	S2L	
F7	F7a	19-400	Fine-grained sandstones	Isotropic hummocky cross stratification, slumping	Branched, horizontal burrows	Suspended load, progressive aggradation storm-modified (or combined) hyperpycnal flows; oscillatory component < unidirectional component	S2h	Sandy, storm-enhanced/combined hyperpycnal flow
	F7b	18-600	Fine-grained sandstones, abundant crinoid columnals	Isotropic hummocky cross stratification	Branched, horizontal burrows	As above; crinoid entrainment; dragging and rolling of crinoid columnals at the base of the suspension cloud; oscillatory component < unidirectional component	S2h	
	F7c	19-103	Fine-grained sandstones	Quasi-planar-lamination	(Cross-cutting), horizontal burrows	As above; unidirectional component > oscillatory component	S2h	
	F7d	36-187	Fine-grained sandstones, abundant crinoid columnals	Quasi-planar-lamination	-	As above; crinoid entrainment; dragging and rolling of crinoid columnals at the base of the suspension cloud; unidirectional component > oscillatory component	S2h	
F8		6-90	Fine-grained sandstones	Wave ripples and wave-ripple cross-lamination	-	Suspended load, remobilisation by wave action	S3w	

						or deposition from oscillatory (i.e. combined) hyperpycnal flows		
F9	F9a		Fine-grained sandstones	Small scale slumps	-	Soft sediment deformation structure (SSDS) triggered by storm wave loading	-	Mass wasting deposits
	F9b		Fine-grained sandstones	Large scale slumps	-	Soft sediment deformation structure (SSDS) triggered by earth quake shock	-	Mass wasting deposits
F10		12-18	Bioclastic lags	Chaotic, crinoid columnals: partial sub-horizontal alignment, brachiopod valves: both convex-up and concave-up	-	Storm surge	-	Tempestite

4.1 Facies

F1a – massive fine-grained sandstones

Description: F1a comprises fine-grained, massive sandstones (5-300 cm), which are commonly amalgamated. Plant detritus and micas are commonly present throughout the sandstone and enriched along bedding planes. Rare ichnofossils (*Paleophycus* isp, *Olenichus* isp) are preserved hypichnially.

Interpretation: Massive fine-grained sandstones suggest deposition within a low energy setting. Such deposits are common in fluvial (e.g. Horn et al., 2018) and marine mouthbar successions (e.g. Feng et al., 2019; J. Zhang et al., 2019). Fine-grained sands are transported as suspended load within hyperpycnal flows, and deposited due to gravitational collapse (Mulder et al., 2003; Zavala et al., 2011a). Zavala et al. (2011a) and Zavala and Pan (2018) describe progressive aggradation from the bottom by sustained hyperpycnal flows which may inhibit the formation of primary sedimentary structures at the basal layer, resulting in the deposition of massive sandstones. Thus, F1a is interpreted as having been deposited by sustained hyperpycnal flows and is correlatable with the S1 facies of Zavala et al. (2011a).

F1b – massive fine-grained sandstone with bioclastic lags

Description: These massive beds (32-250 cm thick, sometimes amalgamated, mica-bearing, abundant plant detritus) contain discrete lags (up to 10 cm) of disaggregated crinoids (sometimes showing subhorizontal alignment). Individual ossicles are also present within the sandstones. Rare horizontal ichnofossils (*Palaeophycus* isp) were also noted.

Interpretation: The presence of bioclastic material within the massive sandstones would suggest possible deposition from hyperpycnal flows (i.e. as in F1a), passing over disarticulated crinoids present on the sea bed. A number of authors (e.g. Ponciano & Della Fávera, 2009; Scheffler et al. 2010; Ponciano *et al.* (2012) have suggested that episodic hyperpycnal flows can entrain the skeletal and disarticulated remains of macroinvertebrates (e.g. crinoids) during periods of low sedimentation rate (Fig. 5). Crinoid stems are transported as bedload by dragging and rolling at the base of the hyperpycnal flows (cf. Ponciano et al., 2012; Ausich, 2021), accumulating within the sand fraction as the flow energy decreases losing the competence to roll/drag them (Zavala & Pan, 2018). Thus, the crinoid fragments were deposited as a result of gravitational segregation within the sustained hyperpycnal flow during periods of flow slackening (Zavala & Pan, 2018). F1b can be considered as a variation of F1a (i.e. crinoid entrainment) and can be correlated with the S1 facies of Zavala et al. (2011a).

202

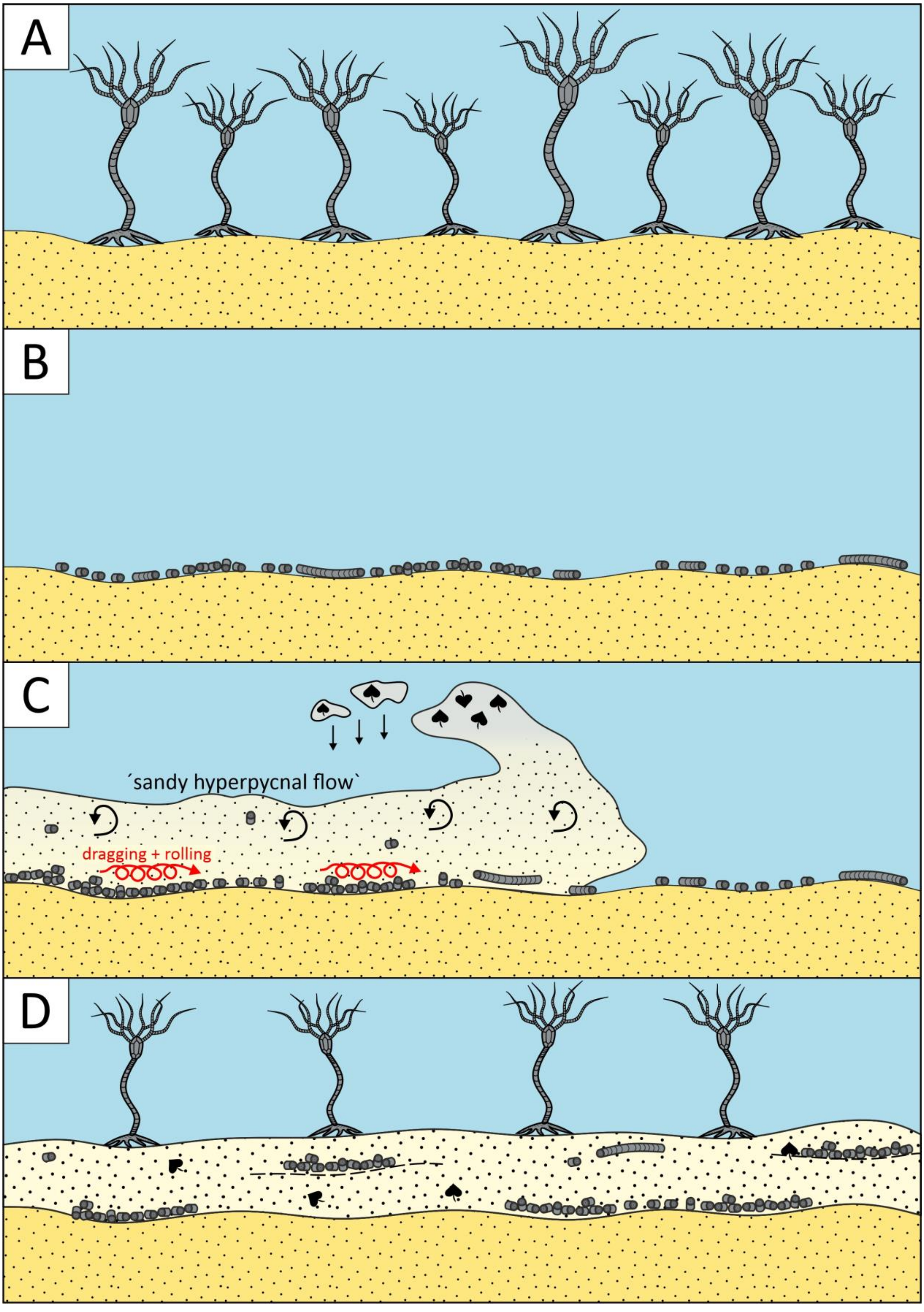

203 *Fig 5: Concept of crinoid entrainment of hyperpycnal flows. A: Colonization of substrate by crinoids. B:*

204 *Death and disarticulation of crinoids during a phase of non-deposition. C: Hyperpycnal flow entrains*

disarticulated crinoids and transports these by dragging and rolling at the base of the flow. D: Recolonization of substrate by crinoids.

<u>F2a – planar-laminated fine-grained sandstones</u>

<u>Description:</u> This facies comprises planar-laminated fine-grained sandstones (5.5-220 cm) which are often amalgamated. Both mica and plant detritus are present. Ichnofossils (*Paleophycus* isp*, Hormosiroidea* isp*)* are preserved hypichnially. Soft-sediment deformation structures (e.g. ball & pillow structures) were also noted.

<u>Interpretation:</u> Planar-laminated fine-grained sandstones are present in a variety of medium to high energy settings including, rivers (Plink-Björklund, 2015), distributary mouth bars in deltaic settings (Eilertsen et al., 2011) and turbiditic successions (Bouma, 1962). Dilute unidirectional flows in the upper flow regime, such as sustained hyperpycnal flows, will produce planar lamination (Simons et al., 1965), due to hydrodynamic fluctuations at the base of the flow (Hesse & Khodabakhsh, 1998) during gravitational collapse of the suspended load (Mulder et al., 2003; Zavala et al., 2011a). Thus, F7 is interpreted to be deposited by a sustained hyperpycnal flow and correlates to the S2 facies of Zavala et al. (2011a).

<u>F2b – planar-laminated fine-grained sandstones with bioclastic lags</u>

<u>Description:</u> F2b comprises planar-laminated fine-grained sandstones with abundant disaggregated crinoid fragments. Individual beds are 17-749 cm thick, and frequently amalgamated. Indeed, internal stratification may appear to be discontinuous. The sands are rich in mica, while plant detritus may also be present.

<u>Interpretation:</u> F2b is a variant of F2a, where unidirectional flows (i.e. hyperpycnal flows) of the upper flow regime, that produce planar lamination (cf. Simons et al., 1965), will entrain crinoid columnals (Ponciano & Della Fávera, 2009; Scheffler et al., 2010; Ponciano et al., 2012). F2b can thus be correlated to the S2 facies of Zavala et al. (2011a).

F3 – fine-grained sandstones with climbing ripples

Description: Facies F3 comprises fine-grained sandstones with climbing ripples. This facies was only encountered *in situ* in one profile, although abundant climbing ripples were also noted in loose material on quarry floors. The measured bed is 101 cm thick, with the ripples inclined upstream at a bedding inclination of up to 20°. Mica is also present.

Interpretation: F3 is interpreted as having been deposited in a low energy setting, where a high suspended sandy load was present (Mulder & Alexander, 2001; Sumner et al., 2008). Such deposits occur in a variety of settings including, lakes (Stanley, 1974), tidal settings (Yokokawa, Kishi, et al., 1995), as well as shelf and (Tanner, 1968) and turbiditic systems (Kuenen & Humbert, 1969; Mulder & Alexander, 2001; Sumner et al., 2008). Within a hyperpycnal system, climbing ripples are interpreted as forming due to a combination of traction and fallout processes, associated with high sedimentation rates during waning turbulent flow stage (Hunter, 1977; Zavala & Pan, 2018), or as part of a channel fill unit deposited from such a waning flow stage. F3 is considered to be equivalent to the S3 facies of Zavala et al. (2011a).

F4 – massive siltstones and mudstones

Description: F4 comprises massive siltstones and claystones (3-50 cm) which sometimes include planar-laminated siltstones and rarely plant detritus. Mica is common and often concentrated along individual bedding planes. Ichnofossils occur as simple (cross-cutting) horizontal burrows (e.g. *Palaeophycus* isp), with some beds completely bioturbated (Bioturbation Index = 4-6).

Interpretation: Such fine-grained deposits are generally deposited in very low energy settings. Typical environments include, muddy tidal flats (Kvale et al., 1989), lagoons (Schaumann et al., 2021), lakes (Marshall & Fletcher, 2002), deltaic interdistributary areas (Hepp et al., 2019), muddy shelves (Safak et al., 2013), as well as deep-marine (Hüneke & Mulder, 2011), and turbiditic settings (Bouma, 1962). Such sediments are commonly interpreted as having been deposited due to normal settling (i.e. fallout) when flow movement completely stops (cf. Zavala & Pan, 2018). Thus, this facies may be useful in recognising the boundaries between different hyperpycnal events. Stow and Wetzel (1990) introduced a new facies type in distal turbiditic systems, termed hemiturbidites. This facies is deposited from a stationary suspension cloud, which is produced from the waning turbidity current. The deposits are described as fine-grained, muddy sediments with aspects which are partly turbiditic and partly hemipelagic, as well as being commonly bioturbated (Stow & Wetzel, 1990). Thus, F4 can be interpreted as hemiturbidites. Since these deposits mark the uppermost part of distal turbiditic deposits (cf. Stow & Wetzel, 1990), they tend to be eroded or deformed (soft-sediment deformation, due to subsequent loading; Allen, 1982) by subsequent turbidity currents (i.e. sustained hyperpycnal flows). Thus, the sediments of facies F4 were deposited as hemiturbidites from sustained hyperpycnal flows, and form part of the uppermost channel infill of distal shelfal hyperpycnal channels. This facies correlates to the S4 facies of Zavala et al. (2011a).

F5– planar-laminated sandstones and siltstones with plant debris

Description: This particular facies includes both planar-laminated, fine-grained sandstones and siltstones (which may be intercalated) in which plant debris is very abundant (Fig. 6). Bedsets vary in thickness from 10-60 cm, with individual beds ranging from a few millimetres to <2 cm. Both plant detritus and micas are present and often concentrated along bedding planes. Rare branched and simple horizontal burrows (*Paleophycus* isp) occur in some siltstone beds.

Interpretation: The sediments of F5 were deposited in a low energy setting. Possible environments include tidal (Visser, 1980), lacustrine (Birks, 2001), and fluvial settings (Wing, 1984) as well as within turbiditic systems (Saller et al., 2006). The ability of hyperpycnal flows to transport extrabasinal plant detritus into marine basins is considered to be a distinctive criterion (Zavala et al. 2011b). So-called lofting rhythmites (after Zavala et al., 2006), which are composed of thin rhythmic sand-silt couplets with abundant plant materials, accumulate from a lofting plume (Zavala et al., 2011a; Zavala et al., 2011b).

A hyperpycnal flow contains freshwater, which is less dense than the ambient water. Due to flow deceleration, a hyperpycnal flow is progressively depleted of its suspended load. Thus, it will consequently lift from the substrate as a result of buoyancy reversal (Sparks et al., 1993; Kneller & Buckee, 2000; Zavala et al., 2011b). A lofting rhythmite will then form from fallout of the suspended silts, fine-grained sands, and plant material, with normal grading often occurring. The plant material will remain in suspension due to its higher buoyancy and will, thus, only be deposited during a subsequent phase of sediment fall-out, thus forming a rhythmite (Zavala et al., 2011b). The deposits of F5 are interpreted as having been deposited, at least partly, from this lofting mechanism and can, thus, be equated with the L facies of Zavala et al. (2011a).

Fig 6: A: Lofting facies (F5 = L) in the Talbecke Ost 2 profile. Note individual beds of discontinuous, massive sandstone beds (red in colour). B: Top of the lofting facies (F5 = L) with several plant fossils. C: Cut through the lofting facies (F5 = L) revealing the layered nature as a rhythmite.

<u>F6 – planar-laminated sandstones with siltstone-levels and plant debris</u>

<u>Description:</u> F6 comprises massive or planar-laminated, mica-rich, fine-grained sandstones with discontinuous, lenses of siltstones and abundant plant debris. Thus, F6 is quite similar to F1/F2 and F5. It can be distinguished from them by the presence of the siltstones. Individual bed thicknesses range from 16 to 25 cm. Plant detritus is, as noted, abundant and is present throughout the beds as well as being concentrated into discrete lenses or laminae and along bedding planes.

<u>Interpretation:</u> The massive or planar-laminated fine-grained sandstones with discontinuous siltstone lenses and abundant plant debris were most possibly deposited in a low to moderate energy setting. While possible settings include tidal (Visser, 1980), lacustrine (Birks, 2001), fluvial (Wing, 1984) or turbiditic environments (Saller et al., 2006), the presence of features of both F1/F2 as well as F5 suggest that F6 is a transitional version of suspended load-transported materials (i.e. sandstones) and fallout-derived sediments (i.e. siltstones). It can be correlated with the S2L facies of Zavala, et al. (2011a).

<u>F7a – hummocky cross stratified fine-grained sandstones</u>

<u>Description:</u> F7a comprises isotropic hummocky cross-stratified, fine-grained sandstones and siltstones (19-400 cm). The heights of the hummocks vary from 19 to 50 cm, with a wavelength of between 40 cm to >200 cm. Amalgamation is very common. Some beds are scoured. Combined-flow ripples (F8) rarely occur at bed tops. Soft-sediment deformation structures (SSDS; F9a) are commonly associated. Mica and plant detritus are present in both the sandstones and the siltstones. Rare *Paleophycus* isp are preserved hypichnially.

<u>Interpretation:</u> While hummocky cross stratification (HCS) is mostly associated with storm-dominated shelves (Chell & Leckie, 1993; Myrow, 2005; Peng et al., 2017; Grundvåg et al., 2021), it has also been

noted in deltaic settings (García-García et al., 2011) and even in fluvial environments (Cotter & Graham, 1991). HCS forms as a result of the superposition of hyperpycnal flows by storm-wave action, creating a combined flow, where the unidirectional flow (i.e. hyperpycnal flow) is modified by an oscillatory component (i.e. storm wave oscillation) (Tinterri, 2011; Jelby et al., 2020; Grundvåg et al., 2021). The facies described herein is similar to that described by Jelby et al. (2020) as a field of: "*complex hummocky cross-stratification generated by highly unsteady wave oscillations and hyperpycnal flows"*. Thus, F7a is believed to have been deposited from a combined flow system and can be correlated with the hyperpycnal systems S2h facies of Zavala et al. (2011a).

F7b – hummocky cross-stratified fine-grained sandstones with bioclastic lags

Description: This facies comprises hummocky cross-stratified sandstones and intercalated siltstones (18-600 cm), with abundant bioclastic lags. Wavelengths vary from 50 cm to >200 cm with heights of 18-40 cm. Amalgamation is very common. Some beds are scoured. Mica and plant detritus are present in both the sandstones and siltstones. Rare *Paleophycus* isp are preserved hypichnially.

Interpretation: This facies is interpreted as a variant of F7a, where a combined flow entrained crinoid columnals. Such crinoid columnals appear at the basis of the beds, often in scours, and their presence is probably related to current winnowing during waning storm conditions (Grundvåg et al., 2021). As a variation of F7a, F7b can be correlated with the S2h facies of Zavala et al. (2011a) as well.

F7c – quasi-planar-laminated fine-grained sandstones

Description: Beds of quasi-planar-laminated fine-grained sandstones range in thickness from 19-103 cm, and show laminae inclinations of between 5°-18°. Mica and plant detritus are distributed throughout the sandstones and often concentrated on bedding planes. Some beds show evidence of coarsening upwards. Bed amalgamation was noted. Some beds are intercalated with HCS (F7a+b) and combined-flow ripples (F8). *Paleophycus* isp, where present, is preserved hypichnially.

Interpretation: Quasi-planar lamination (QPL) was first reported by Arnott (1993) who also noted the linkage between such beds and those exhibiting hummocky cross stratification. QPL develops under high-energy combined-flow conditions, where a weak (to possibly strong) unidirectional current combines with a long-period, high-velocity oscillatory current. In addition, QPL is believed to be the transitional facies towards isotropic or oscillatory forms of HCS, where the unidirectional component is stronger than it is during the formation of HCS (Arnott, 1993; Dyson, 1996; Tavares Calandrini de Azevedo et al., 2024). This is possibly related to the waxing and waning (i.e. pulsating) of the hyperpycnal discharge. Thus, F7c is interpreted as a variation of F7a, and could, therefore, be correlated with the S2h facies of Zavala et al. (2011a).

F7d – quasi-planar-laminated fine-grained sandstones with bioclastic lags

Description: F7d is derived from quasi-planar-laminated fine-grained sandstones with bioclastic lags (36-187 cm). Amalgamation is common. Laminae inclination ranges from 10°-15°. Some beds show a coarsening upwards trend or bioclastic lags in scours at the bed bases.

Interpretation: Facies F7d can be considered to be a variant of F7c, where a combined flow, with a strong unidirectional component, entrained crinoid columnals. Thus, F7d can also be related to the S2h facies of Zavala et al. (2011a) as well.

F8 – fine-grained sandstones with combined-flow ripples

Description: F8 comprises fine-grained sandstones (6-90 cm) with ripples and/or ripple cross-laminated sandstones which are often mica rich and amalgamated. The height of the ripples varies from 0.5-1 cm, while the wavelengths range from 5-18 cm. Ripples are asymmetrical with both rounded and occasionally sharp crests. Foresets exhibit a sigmoid configuration with convex-up lee and stoss sides (Fig. 7). Thus, the ripples are identified as combined-flow ripples. This facies is commonly intercalated with or within the HCS sandstones of F7a+b.

Interpretation: Fine-grained sandstones with combined-flow ripples are interpreted to have been deposited from combined flows, where a unidirectional component is superimposed by a (storm)wave-induced oscillatory component (Yokokawa, Masuda, & Endo, 1995; Yamaguchi & Sekiguchi, 2010; Basilici et al., 2012). The facies was deposited from oscillatory-dominated (i.e. combined) hyperpycnal flows (cf. Zavala & Pan, 2018), and, therefore, correlates to the S3w facies of the proposed genetic facies tract of hyperpycnal systems of Zavala et al. (2011a).

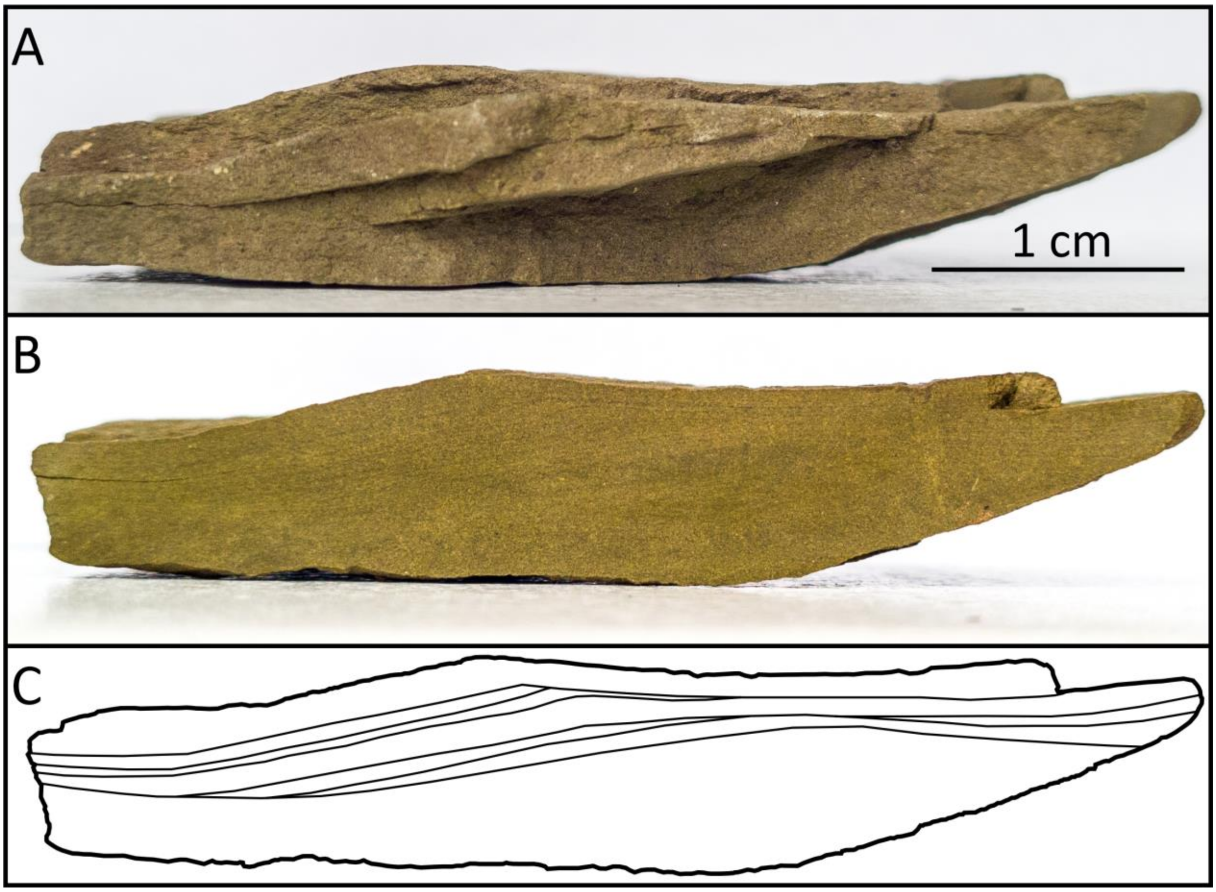

Fig 7: A: Handspecimen of a combined flow ripple. B: The handspecimen was cut and polished to reveal the sigmoid configuration of the laminae. C: Redrawing of the sigmoid-configurated laminae.

<u>F9a – small-scale slumps</u>

<u>Description:</u> Within the HCS sandstones of F8a+b, small-scale slumps occur frequently. These slumped beds vary in thickness from 5 to 30 cm. Lithologically, these slumps comprise fine-grained sands.

<u>Interpretation:</u> Since the slumps are associated with HCS, which is indicative of storm activity, deformation most probably resulted from storm wave loading (see Owen & Moretti, 2011). Storm waves can induce liquidization (liquefaction and/or fluidization) in saturated and unconsolidated sediments (Allen, 1982; Q. Zhang & Suhayda, 1994; Molina et al., 1998; Alfaro et al., 2002). Three processes are associated with this: (1) remobilization of sediments during storms may result in

overloading (Kerr & Eyles, 1991; Molina et al., 1997); (2) impulsive loading (*sensu* Owen, 1987), due to direct impact of breaking waves in shallow marine environments (Henkel, 1970; Dalrymple, 1979); and, (3) increasing interstitial pore pressure due to cyclic stresses caused by pressure differences between the crests and troughs of successive wave trains during storms (Allen, 1982; Owen, 1987). Due to the continuous, combined-hyperpycnal deposition of the deposits above the slumps (i.e. no storm surge deposits), and the position of the hyperpycnal-fed system on the shelf with a putative water column of tens to hundreds of metres, the later triggering mechanism (3) is favoured herein.

F9b – large-scale slumps

Description: In the abandoned Unnenberg quarry an up to 2.6 m thick slump crops out (Fig. 8; for a detailed sketch see Jux, 1960, pp. 208–209). The slumped horizon can be traced for c. 25 m. It cuts down into the underlying beds to a depth of c. 2 m. The slumped sediments comprise mainly fine-grained sandstones. Other similar and large-scale slumps (0.5-1.5 m) occur randomly within the measured profiles (e.g. Fig. 9-10).

Interpretation: Larger-scale slumps can be induced by a variety of mechanisms including volcanic or tectonic activity. Extension-related volcanics have been described for the Middle Devonian in the Bergisches Land, Sauerland and the Lahn-Dill region (Meyer, 1981; Werner, 1988; Nesbor, 2004; Königshof et al., 2010; Schnapperelle et al., 2021). Furthermore, both Plessmann and Spaeth (1971) and Werner (1988) describe the presence of clastic dykes in the Wissenbach Formation (Upper Eifelian) near Menden (northern Sauerland) which they suggested were formed during earthquakes (although they may also result from overloading (Onorato et al., 2016) or storm wave loading (Molina et al., 1997). The Wissenbach Formation represents the neritic continuum ("Hercynian facies"; see Jansen, 2016) of the depositional basin of the Unnenberg Formation (Thienhaus, 1940; Spriestersbach, 1942; von Kamp et al., 2017). Thus, tectonic activity alone, or in combination with storm wave loading, is a possible mechanism for the large-scale slumping in the Unnenberg Formation.

F10 – bioclastic lags

Description: The bioclastic lags comprise mainly disaggregated and broken fragments of crinoids, i.e. crinoid columnals. Very rare brachiopod valves were also noted. The lags are 12-18 cm thick. Individual crinoid columnals show partial sub-horizontal alignment. The very rare brachiopod valves are preserved in both convex- and concave-up positions. The bioclastic fragments are preserved within a very fine- to fine-grained sandy matrix.

Interpretation: Bioclastic lags are interpreted as having been deposited in a high energy setting. Such lags are described from a variety of depositional settings, including tidal channels (Flemming et al., 1992), storm-dominated shelfs and coasts (Banerjee, 1981; Mohseni & Al-Aasm, 2004), estuaries (Anderson & McBride, 1996), deltas (Longhitano et al., 2010), lakes (Michael J. Soreghan, 1996) and turbidite systems (Middleton, 1967) (also termed bioclastic turbidites; see Mehrtens, 1988). The main depositional process associated with their deposition are storm surges, where bioclastic material is first churned up and then redeposited as the storm abates. The process was originally termed storm turbulence (or storm-induced turbulence) (see Schultze et al., 2020). Thus, these deposits are considered to represent a tempestite facies within the depositional environment.

Fig 8: Hagen 2 quarry near Gummersbach. Amalgamated sandstones appear as tabular bodies, which are traceable over tens of metres. The quarry is approximately 20 metres high. B: Tempestite facies with disarticulated crinoid columnals (i.e. bioclastic lag) from the Hagen 2 quarry. C: Climbing ripples from the Hagen 2 quarry. D: Ball and pillow structure from the Talbecke Ost 2 Nebenbruch profile. E: Slumped interval from the Unnenberg quarry (Unnenberg lower level profile). F: Hummocky cross stratification with small scale slump at the base of the interval at the Unnenberg upper level profile.

<u>4.2 Facies associations</u>

The 10 facies recognised and discussed above were subsequently grouped into three facies associations. Each of these represents part of a hyperpycnal-fed, foredeltaic environment, which developed either as a lobe system or within a ramp setting, depending on storm activity.

FA1 – proximal hyperpycnal subaqueous delta lobe facies association

Description: This facies association comprises thick (up to 7 m) amalgamated, tabular, fine-grained sandstones (F1-F4), which are capped by muddy deposits of the hyperpycnal lofting plumes (F5). Thereby, massive sandstones (F1/S1) are intercalating with planar-laminated sandstones (F2/S2) and rippled sandstones (F3/S3, F8/S3w). Individual beds/units are traceable over tens of metres.

Interpretation: The deposits of fluctuating hyperpycnal flows form cyclic (albeit complex) sequences comprising massive, laminated and climbing ripple sandstones (Zavala & Pan, 2018). Zavala et al. (2011b) describe the process of lofting in hyperpycnal flows as a result of flow velocity deacceleration. Lofting plumes develop either in the distal parts of hyperpycnal flows or along channel margins (Zavalabet al., 2011a; Zavala et al., 2011b). Thus, the facies association is interpreted to represent proximal, shelfal lobes of a hyperpycnal subaqueous delta (HSD).

FA2 – distal hyperpycnal subaqueous delta lobe facies association

Description: FA2 comprises stacked associations (up to 3.5 m) of tabular, thin-bedded, fine-grained sandstones (F1-F4) and mudstones (F5-F6). The sandstones comprise a variety of sedimentary structures, including planar-lamination, ripple-cross lamination, and normal grading. Within the facies association, fine-grained sandstones are overlain by mudstones or graded beds (fS-vfS). FA2 is typically enriched in both plant remains and mica towards the top of the facies association.

Interpretation: The deposits of FA2 are broadly similarly to those of FA1, though the individual beds and bedsets are thinner in the former. Thus, the FA2 units represent a more distal depositional setting towards FA1. Therefore, the deposits are interpreted as distal, shelfal lobes of a hyperpycnal subaqueous delta (HSD).

FA3 – hyperpycnal littoral delta mid-ramp facies association

Description: Fine-grained sandstone beds and bedsets comprising HCS, QPL and combined-flow ripples (F7a-d/S2h, F8/S3w) alternate with planar-laminated sandstones (F2/S2). Tempestites (F10) often appear at the base of the FA3. Graded sandstones of F4/S4 cap the FA3. FA3 exhibits tabular geometries.

Interpretation: The alternation of HCS and QPL with planar-laminated sandstones was described by Lamb et al. (2008) as the result of pulsating wave-enhanced (or combined) hyperpycnal flows. Thereby, hyperpycnal flows are superimposed by storm-wave energy, which aids the distribution of the fine-grained sediments (i.e. sand-silt-clay) across large areas (hundreds of km's) due to the construction of a low gradient, progradational, clastic, deltaic ramp (=hyperpycnal littoral delta of Zavala et al. (2021). According to Zavala et al. (2021) and Zavala et al. (2024), such hyperpycnal littoral deltas are partially equivalent to 'subaqueous deltas' (cf. Kuehl et al., 1986), ramp deltas (cf. Overeem et al., 2003), prodeltaic shelves (cf. Bhattacharya & MacEachern, 2009), muddy prodeltaic hyperpycnites (cf. Wilson & Schieber, 2014), river-dominated deltaic parasequences (cf. Ahmed et al., 2014), storm-flood-dominated deltas (cf. Lin & Bhattacharya, 2021) and shelf hyperpycnites (cf. Olariu, 2023). Thus, FA3 represents the mid-ramp area of the hyperpycnal littoral delta, where sediments accumulate as a result of traction-plus-fallout from unconfined wave-enhanced (or combined) hyperpycnal flows (Irastorza et al., 2021)

4.3 Elementary depositional sequences (EDS)

Elementary depositional sequences (*sensu* Mutti et al., 2000) are 1.5-11 m thick successions of shallowing upwards beds and bedsets, and their presence within the Unnenberg Formation would suggest that the hyperpycnal-deltaic system was broadly progradational. However, two EDS within the formation (Fig. 9-10) exhibit deepening upward configurations (i.e. retrogradational phases).

Each EDS (both progradational and retrogradational) is bounded at its base by the occurrence of entrained crinoids above an erosive surface. As mentioned above, episodic hyperpycnal flows are able to entrain skeletal remains of macroinvertebrates (i.e. crinoids) which completely disarticulated during periods of low sedimentation rate, suggesting a phase of non-deposition (Ponciano & Della Fávera, 2009; Scheffler et al., 2010; Ponciano et al., 2012). Such bioclast-rich beds can, therefore, be used as sequence boundaries (cf. Davies et al., 1989; Banerjee & Kidwell, 1991; Kondo et al., 1998). Shallowing-upward sequences comprise either bedsets of a single facies association or of alternating facies associations, suggesting rapid shifting and stacking of the HSD-lobes within the HLD-ramp setting. Moving up in the stratigraphy, each EDS is bounded by condensed intervals of bioturbated sediments of F4 (S4, after Zavala et al., 2011a) or F5 (L, after Zavala et al., 2011a), which mark the sequence stratigraphic boundary , or again by a basal erosive surface with entrained crinoids of the next EDS.

In contrast to parasequences, which are controlled by relatively rapid sea-level rises (cf. van Wagoner et al., 1988; Arnott, 1995; van Wagoner et al., 1996), EDS are allocyclic controlled by long-term climate changes (e.g. increased runoff by increased precipitation during wet phases), and, therefore, by Milankovitch cyclicity (Mutti et al., 2000). Thus, climate-controlled hyperpycnal systems may show a progradational or retrogradational pattern, entirely independent of a rising or falling sea level.

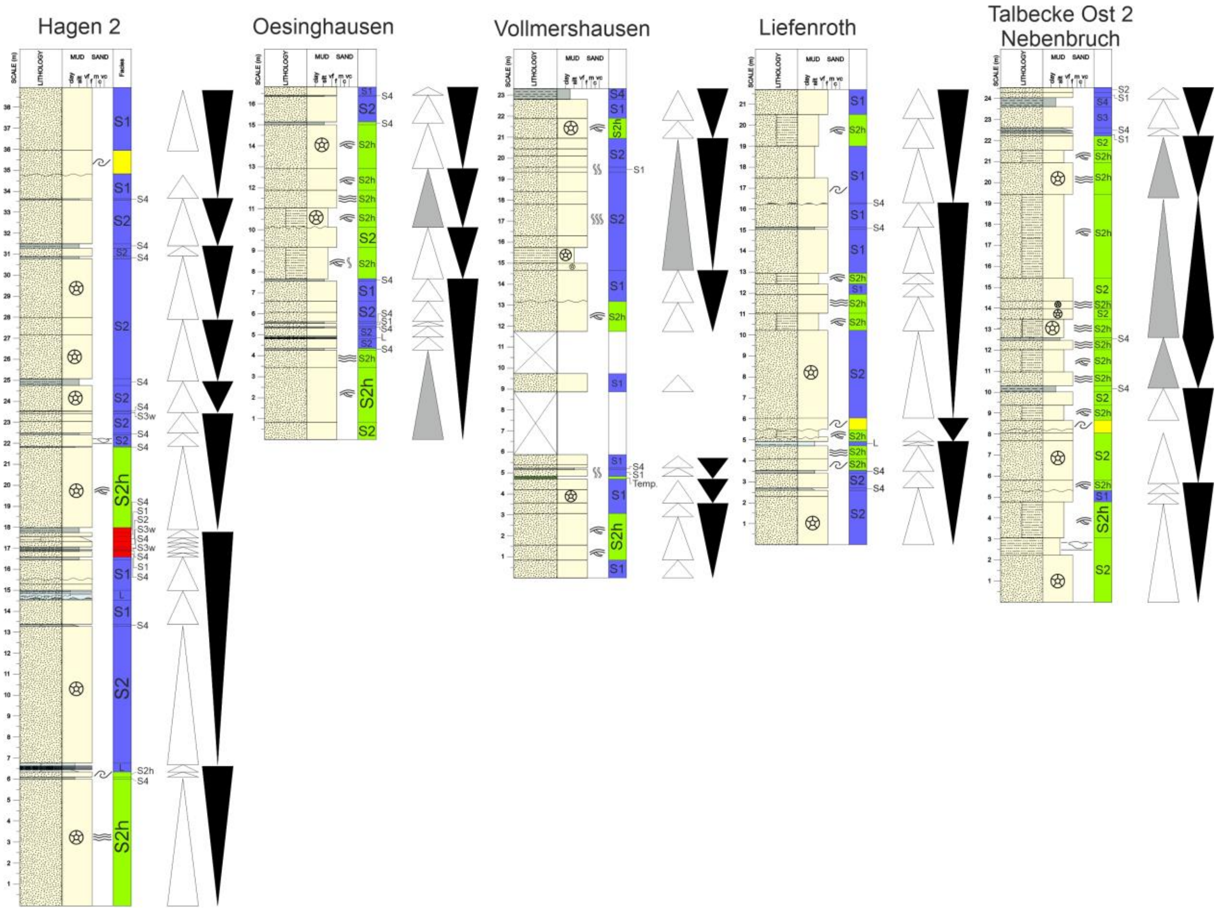

Fig 9: Profiles of the Unnenberg Fm. For locality, see Fig 3. For legend, see Fig 9.

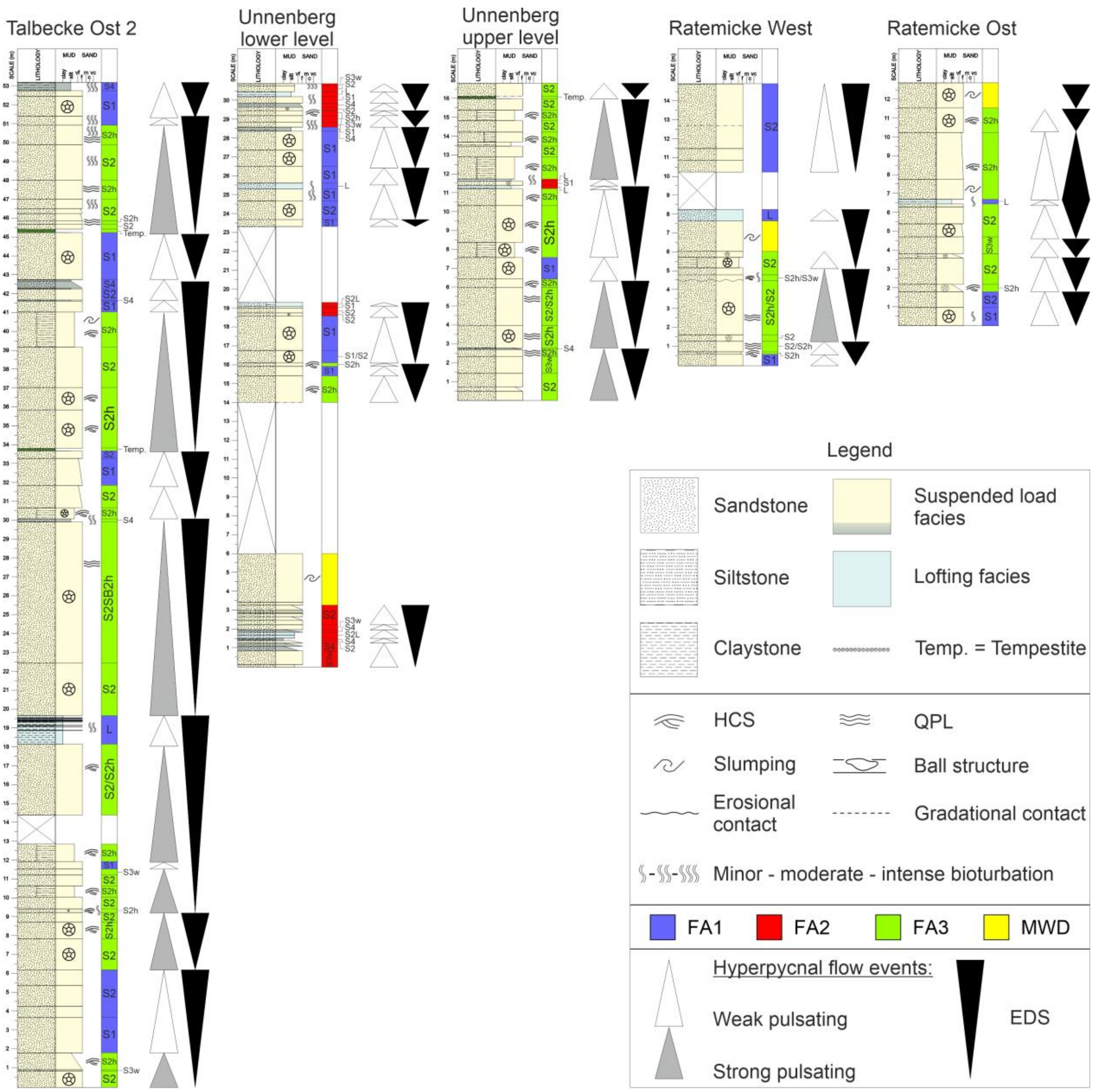

Fig 10: Profiles of the Unnenberg Fm. For locality, see Fig 3.

5. Discussion

5.1 Depositional model and paleogeographic reconstruction

Based on the high-resolution facies analysis of ten profiles from the Unnenberg Formation near Gummersbach, with a combined length of c. 255 m, it was shown that the Rheic Shelf was supplied with large amounts of fine-grained sediments from a complex hyperpycnal, deltaic system. This system was part of a larger integrated, delta-shelf-basin depositional system, which will be described below (Fig. 11).

The interpretation of a linked delta-shelf-basin system is partly based on the early work of Pfeiffer (1938) and Thienhaus (1940), who suggested that the deltaic deposits of the Brandenberg Formation were related to the deposits of the Unnenberg Formation, although the precise nature of the relationship between the two areas was unclear. A number of authors including, Pfeiffer (1938), Langenstrassen et al. (1979), Langenstrassen (1983) and Reuter (1993) suggested that the deposits of the Brandenberg Formation were deposited in a high-destruction delta system, one where strong erosional forces (i.e. wave action and/or tides) were active. A large deltaic lobe, related to the main deltaic system, developed in the Wuppertal-Beyenburg region (Pfeiffer, 1938; Langenstrassen et al., 1979) while the adjacent coastline, comprising an alluvial plain with marine, brackish and limnic sub-environments (Pfeiffer, 1938; Langenstrassen, 1983; Otto, 1999; Gosny, 2010), was located in the Düsseldorf-Wuppertal-Iserlohn region (c. 30-55 km to the NW of the Unnenberg Formation outcrops). According to Mustafa (1975, 1978a, 1978b), Schweitzer (1990) and Koch (2023), these coastlands were covered by some of the earliest land plants with species of *Psilophyton, Pseudosporochnales* and *Aneurophytales* all noted.

Subsequent work on the depositional environment of the Unnenberg Formation suggested a reinterpretation as a tidal flat system (Grabert, 1971), a storm-dominated muddy shelf environment with shoal-like bodies or a barrier island system (Bininda, 1980), a prodeltaic (or foredelta) environment (Jux, 1983), or prograding, storm surge-generated sand bars (Ribbert & Baumgarten, 2012; Ribbert, 2013). However, the results of this current work would suggest that the deposition of the Unnenberg Formation was either from sustained hyperpycnal flows, which formed the shelfal channels and lobes, or from wave-enhanced (or combined) hyperpycnal flows, which constructed a deltaic ramp. The deposits of the Unnenberg Formation primarily accumulated in the area of Gummersbach, where thick-bedded sandstone bodies are dominant. Moving away from this area, i.e. to the W/SW (Dietz & Fuchs, 1935), the S/SE (Fuchs & Schmidt, 1928; Ribbert, 2013), and the E (Clausen, 1978; Ziegler, 1978; Thünker, 2011) the sandstone beds are markedly thinner or may even pinch out. Indeed, these areas lateral to the Gummersbach region tend to be dominated by mudstones.

Work on the Lennehelle Formation (e.g. Langenstrassen (1972), Clausen (1978), Ziegler (1978), Thünker (2011), von Kamp et al. (2017) and Ribbert et al. (2017) established a correlation with the sediments of the Unneberg Formation, suggesting the possible genetic linkage of the two formations, and thereby, the depositional systems. This current study proposes that the sandstones of the Lennehelle Formation are turbidites, and that they accumulated as deep-marine lobes at the base of the continental slope. Such surge-like turbidity currents may have originally been hyperpycnal flows which changed as a result of flow transformation.

Three other formations, namely, the Ramsbeck (Thienhaus 1940), Asten (Kunert 1965), and Raumland (Ribbert *et al.* (2017) formations, crop out in the eastern Sauerland region (Ostsauerland anticline), c. 45-60 km to the SE of outcropping strata of the Unnenberg Formation, and can also be correlated with the deposits of Unnenberg and Lennehelle Formations. The most distal deposits of this proposed depositional system are believed to be represented by the Eifel-Quarzit in the Wittgenstein and Dill synclines (c. 45-60 km to the SE of the Unnenberg Formation outcrops) (Klitzsch, 1959; Lippert et al., 1970). The sediments of the aforementioned formations accumulated in deep-marine (sub-)basins of the Rhenoherzynian Ocean (cf. Krebs, 1979). The formations are all characterised by successions of mudstones with intercalated sandstone beds, these latter interpreted as turbidites (Ribbert et al., 2017).

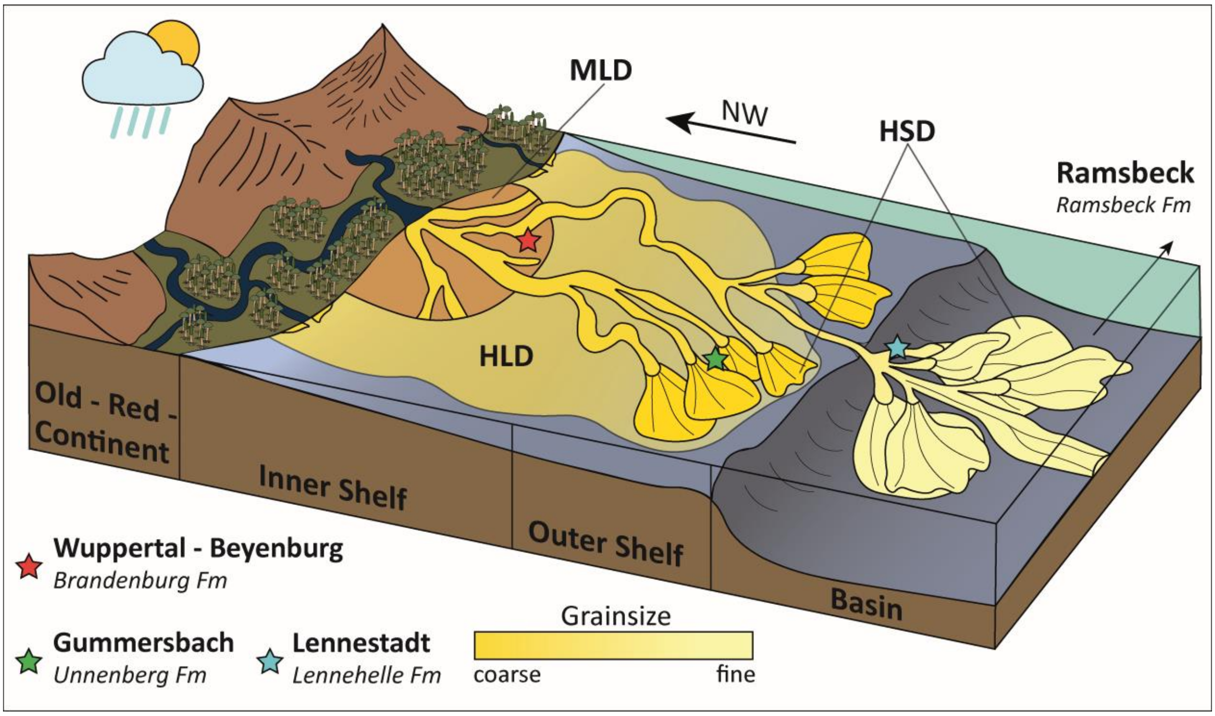

Fig 11: Schematic depositional model of the hyperpycnal subaqueous delta (HSD) and hyperpycnal littoral delta (HLD) of the Unnenberg Fm and both its connected coastal, deltaic (marine littoral delta = MLD; Brandenberg Fm) and deep marine (Lennehelle Fm, Ramsbeck Fm) continuum, which was controlled by monsoonal activity.

5.2 Monsoonal drivers of hyperpycnal flow origin

Monsoons are able to trigger hyperpycnal flows by either drastically increasing erosion during monsoon rains, or by the dilution of seawater during periods of increased precipitation/runoff (Mulder et al., 2003; Bourget et al., 2010; Wang et al., 2010; Zheng et al., 2014). During the Eifelian, monsoon-like dynamics were controlled by a half-precession cycle of 9.8 kyr and a precession cycle of 18 kyr (de Vleeschouwer et al., 2012), resulting in wet/very wet phases separated by dry phases (Cecil, 1990; Streel, 2000) and, thus, regulating the detrital influx (by precipitation and wind) onto the Rheic Shelf (Witzke & Heckel, 1988; de Vleeschouwer et al., 2012; Da Silva et al., 2013; de Vleeschouwer et al., 2013; 2017). During monsoonal periods, winds will drastically increase wave height (Amrutha et al., 2015; Andutta et al., 2019). Thus, oscillatory flow components are superimposed on the putative hyperpycnal flows, allowing the formation of combined flows (cf. Tinterri, 2011; Jelby et al., 2020;

Grundvåg et al., 2021). Therefore, monsoonal dynamics during the upper Eifelan would appear to be a feasible triggering mechanism for hyperpycnal flows within the depositional setting.

If the EDS are considered to be equivalent of the proposed half-precession cycle of 9.8 kyr of de Vleeschouwer et al. (2012), they could be classified as a fifth-order sequence. Thereby, the averaged sedimentation rate of the EDS (thicknesses between 1.5 to 11 m) could be expressed as 0.15 - 1.12 m/kyr. However, it should be noted that such a sedimentation rate is merely an estimate, since factors such as compaction, bioturbation, hiatuses are not considered herein. However, if this sedimentation rate is compared with the average sedimentation of the Middle Devonian of the Eastern Rhenish Massif of 0.3 m/kyr (Langenstrassen et al., 1979), the averaged sedimentation rate of the Middle Eifelian to Lower Givetain Eifel region of 0.13 m/kyr (Weddige, 1977; Kaufmann, 2006; de Vleeschouwer et al., 2012), and the sedimentation rate of the hyperpycnal-fed Bengal fan of 1.2 m/kyr (Worm et al., 1998), the values do not appear to be beyond the realm of possibility. This would suggest that the sequence stratigraphic interpretation is certainly realistic.

6. Conclusion

The depositional setting of the Bergisches Land and Sauerland (Rhenish Massif, Germany) in Eifelian (Middle Devonian) times was characterized by an extensive, hyperpycnal-fed, foredaltaic environment. This showed extensive development of hyperpycnites (derived from sandy hyperpycnal flows and sandy, storm-enhanced/combined hyperpycnal flows), hemiturbidites (transformed from hyperpycnal flows), tempestites and mass wasted deposits (slumps), all of which were deposited on the evolving Rheic Shelf. Elementary depositional sequences with an estimated sedimentation rate of 0.15 - 1.12 m/kyr suggest a progradational configuration of the system, that was probably driven by monsoonal activity, which was controlled by a half-precession cycle of 9.8 kyr. During peak monsoon activity, oscillatory flow components were superimposed on the putative hyperpycnal flows, allowing the formation of combined flows. This resulted in the construction of a low gradient, progradational, clastic, deltaic ramp (=hyperpycnal littoral delta, Zavala et al. (2021). Hyperpycnal flows which developed during phases of low or non-storm activity led to the construction of extensive shelfal lobes (=hyperpycnal subaqueous delta, Zavala et al. (2021). The present system is part of a larger delta-shelf-basin system which extended from the deltaic coastline (Brandenburg Formation), across the shelf (Unnenberg Formation) and the shelf slope (Lennehelle Formation) towards the nereitic basin (Ramsbeck Formation, Asten Formation, Raumland Formation, Eifel-Quarzit). Sandstones which accumulated at the base of the continental slope and within the neritic basin are interpreted as deep-marine lobes, which were fed by surge-like turbidity currents that may have originally been hyperpycnal flows which changed as a result of flow transformation. Thus, hyperpycnal flows played a major role in shuttling sandy material across the shelf of the Rhenoherzynian Ocean during the Eifelian. Such hyperpycnal flow-dominated systems are in important mechanism for the transport and deposition of large volumes of sediment onto continental shelfs and beyond (e.g. Mutti et al., 2003; Pattison, 2005; Steel et al., 2018; Jelby et al., 2020; Grundvåg et al., 2023).

A number of criteria for the recognition of hyperpycnal flow activity (amplified by monsoonal activity) in the Bergisches Land and Sauerland (Rhenish Massif, Germany), were noted. These include the presence of:

1. Lofting rhythmites containing abundant extrabasinal plant detritus as recognized in several locations of the Unnenberg Formation. In general, the deposits described herein are typically enriched in plant material suggesting a sustained connection of the depositional system on the shelf with a riverine, land-derived source.
2. Hummocky cross stratification which formed as a result of the superposition of a unidirectional flow (i.e. hyperpycnal flow) by an oscillatory component (i.e. storm wave oscillation). Hummocky cross-stratified sandstones are a dominant lithology across the region.
3. Cyclic (albeit complex) sequences comprising tabular, massive, planar-laminated, graded and climbing ripple sandstones which suggest that deposition occurred from fluctuating hyperpycnal flows.

4. Hyperpycnal flows which were able to entrain disarticulated crinoid columnals and stems, suggesting a prior phase of non-deposition. Thus, such intervals could be used as a lower sequence stratigraphic boundary. An upper sequence stratigraphic boundary would have been represented by either lofted intervals or hemiturbidites, both of which mark the final phase of hyperpycnal deposition.

7. Acknowledgment

We would like to express our sincere thanks to Prof. Dr. C. März, whose very thoughtful and always helpful suggestions have significantly improved the manuscript and raised it to a higher scientific level. Further we want to thank L. Schenk-Schlautmann, without whom the collection of the profiles would not have been possible. Thanks to R. Schwarz and N. Schmülling, who both helped in cutting and polishing samples.

8. Conflict of Interest

We declare no conflict of interest.

9. Data Availability

A version of this manuscript will be available on EarthArXiv. Raw Data is available within the supplementary materials.

10. Author Contribution

Conceptualisation and Methodology: RMS; Formal analysis and Investigation: RMS; Writing – original draft: RMS; Writing – review and editing: TM; Visualisation: RMS; Supervision: TM.

References

Ahmed, S., Bhattacharya, J. P., Garza, D. E., & Li, Y. (2014). Facies Architecture and Stratigraphic Evolution of A River-Dominated Delta Front, Turonian Ferron Sandstone, Utah, U.S.A. *Journal of Sedimentary Research*, *84*(2), 97–121. https://doi.org/10.2110/jsr.2014.6

Alfaro, P., Delgado, J., Estévez, A., Molina, J., Moretti, M., & Soria, J. (2002). Liquefaction and fluidization structures in Messinian storm deposits (Bajo Segura Basin, Betic Cordillera, southern Spain). *Geologische Rundschau*, *91*(3), 505–513. https://doi.org/10.1007/s00531-001-0241-z

Allen, J. R. L. (1982). *Sedimentary structures, their character and physical basis*. *Developments in Sedimentology: 30B*. Elsevier Scientific Pub. Co. https://ebookcentral.proquest.com/lib/kxp/detail.action?docID=405222

Amrutha, M. M., Sanil Kumar, V., Sharma, S., Singh, J., Gowthaman, R., & Kankara, R. S. (2015). Characteristics of shallow water waves off the central west coast of India before, during and after the onset of the Indian summer monsoon. *Ocean Engineering*, *107*, 259–270. https://doi.org/10.1016/j.oceaneng.2015.07.061

Anderson, L. C., & McBride, R. A. (1996). Taphonomic and Paleoenvironmental Evidence of Holocene Shell-Bed Genesis and History on the Northeastern Gulf of Mexico Shelf. *PALAIOS*, *11*(6), 532. https://doi.org/10.2307/3515189

Andutta, F. P., Patterson, R. G., & Wang, X. H. (2019). Monsoon driven waves superpose the effect from macro-tidal currents on sediment resuspension and distribution. *Estuarine, Coastal and Shelf Science*, *223*, 85–93. https://doi.org/10.1016/j.ecss.2019.04.036

Arnott, R. W. C. (1993). Quasi-Planar-Laminated Sandstone Beds of the Lower Cretaceous Bootlegger Member, North-Central Montana: Evidence of Combined-Flow Sedimentation. *Journal of Sedimentary Research*, *63*, 488–494. https://doi.org/10.1306/D4267B31-2B26-11D7-8648000102C1865D

Arnott, R. W. C. (1995). The Parasequence Definition--Are Transgressive Deposits Inadequately Addressed? *Journal of Sedimentary Research*, *Vol. 65B.* https://doi.org/10.1306/D42681D0-2B26-11D7-8648000102C1865D

Ausich, W. I. (2021). *Disarticulation and Preservation of Fossil Echinoderms: Recognition of Ecological-Time Information in the Echinoderm Fossil Record*. Cambridge University Press. https://doi.org/10.1017/9781108893374

Banerjee, I. (1981). Storm lag and related facies of the bioclastic limestones of the Eze-Aku Formation (Turonian), Nigeria. *Sedimentary Geology*, *30*(1-2), 133–147. https://doi.org/10.1016/0037-0738%2881%2990016-6

Banerjee, I., & Kidwell, S. M. (1991). Significance of molluscan shell beds in sequence stratigraphy: an example from the Lower Cretaceous Mannville Group of Canada 1. *Sedimentology*, *38*(5), 913–934. https://doi.org/10.1111/j.1365-3091.1991.tb01879.x

Basilici, G., Luca, P. H. V. de, & Poiré, D. G. (2012). Hummocky cross-stratification-like structures and combined-flow ripples in the Punta Negra Formation (Lower-Middle Devonian, Argentine Precordillera): A turbiditic deep-water or storm-dominated prodelta inner-shelf system? *Sedimentary Geology*, *267-268*, 73–92. https://doi.org/10.1016/j.sedgeo.2012.05.012

Becker, R. T, Marshall, J., Da Silva, A.-C, Agterberg, F. P., Gradstein, F. M., & Ogg, J. G. (2020). The Devonian Period. In *Geologic Time Scale 2020* (pp. 733–810). Elsevier. https://doi.org/10.1016/B978-0-12-824360-2.00022-X

Beelen, D., & Wood, L. J. (2023). Predicting bottom current deposition and erosion on the ocean floor. *Basin Research*, Article bre.12788. Advance online publication. https://doi.org/10.1111/bre.12788

Bhattacharya, J. P., & MacEachern, J. A. (2009). Hyperpycnal Rivers and Prodeltaic Shelves in the Cretaceous Seaway of North America. *Journal of Sedimentary Research*, *79*(4), 184–209. https://doi.org/10.2110/jsr.2009.026

Bininda, R. (1980). An offshore-coastal sand sequence in the Unnenberg-Schichten (Middle Devonian) near Becke, northern Rheinisches Schiefergebirge. In K. J. Hsü & A. Matter (Eds.), *International Association of Sedimentologists - 1st European regional Meeting 1980 Bochum (Germany): Abstracts* (pp. 86–88).

Birks, H. H. (2001). Plant Macrofossils. In J. P. Smol, H. J. B. Birks, W. M. Last, R. S. Bradley, & K. Alverson (Eds.), *Developments in Paleoenvironmental Research: Vol. 3. Terrestrial, algal, and siliceous indicators* (Vol. 3, pp. 49–74). Kluwer. https://doi.org/10.1007/0-306-47668-1_4

Bouma, A. H. (1962). *Sedimentology of some Flysch deposits: a graphic approach to facies interpretation*. Elsevier Pub. Co.

Bourget, J., Zaragosi, S., Mulder, T, Schneider, J.-L., Garlan, T., van Toer, A., Mas, V., & Ellouz-Zimmermann, N. (2010). Hyperpycnal-fed turbidite lobe architecture and recent sedimentary processes: A case study from the Al Batha turbidite system, Oman margin. *Sedimentary Geology*, *229*(3), 144–159. https://doi.org/10.1016/j.sedgeo.2009.03.009

Cecil, C. B. (1990). Paleoclimate controls on stratigraphic repetition of chemical and siliciclastic rocks. *Geology*, *18*(6), 533. https://doi.org/10.1130/0091-7613(1990)018%3C0533:PCOSRO%3E2.3.CO;2

Chell, R. J., & Leckie, D. A. (1993). Hummocky cross-stratification. In V. P. Wright (Ed.), *Sedimentology review/1.* Blackwell Scientific Publications.

Clausen, C.-D. (1978). *Erläuterungen zu Blatt 4814 Lennestadt*. Geologisches Landesamt Nordrhein-Westfalen.

Cotter, E., & Graham, J. R. (1991). Coastal plain sedimentation in the late Devonian of Southern Ireland; hummocky cross-stratification in fluvial deposits? *Sedimentary Geology*, *72*(3-4), 201–224. https://doi.org/10.1016/0037-0738(91)90012-3

Da Silva, A. C., de Vleeschouwer, D., Boulvain, F., Claeys, P, Fagel, N., Humblet, M., Mabille, C., Michel, J., Sardar Abadi, M., Pas, D., & Dekkers, M. J. (2013). Magnetic susceptibility as a high-resolution correlation tool and as a climatic proxy in Paleozoic rocks – Merits and pitfalls: Examples from the Devonian in Belgium. *Marine and Petroleum Geology*, *46*, 173–189. https://doi.org/10.1016/j.marpetgeo.2013.06.012

Dalrymple, R. W. (1979). Wave-induced liquefaction: a modern example from the Bay of Fundy. *Sedimentology*, *26*(6), 835–844. https://doi.org/10.1111/j.1365-3091.1979.tb00976.x

Davies, D. J., Powell, E. N., & Stanton, R. J. (1989). Taphonomic signature as a function of environmental process: Shells and shell beds in a hurricane-influenced inlet on the Texas coast. *Palaeogeography, Palaeoclimatology, Palaeoecology*, *72*, 317–356. https://doi.org/10.1016/0031-0182(89)90150-8

de Vleeschouwer, D., Da Silva, A. C., Boulvain, F., Crucifix, M., & Claeys, P (2012). Precessional and half-precessional climate forcing of Mid-Devonian monsoon-like dynamics. *Climate of the Past*, *8*(1), 337–351. https://doi.org/10.5194/cp-8-337-2012

de Vleeschouwer, D., Da Silva, A.-C, Sinnesael, M., Chen, D., Day, J. E., Whalen, M. T., Guo, Z., & Claeys, P (2017). Timing and pacing of the Late Devonian mass extinction event regulated by eccentricity and obliquity. *Nature Communications*, *8*(1), 2268. https://doi.org/10.1038/s41467-017-02407-1

de Vleeschouwer, D., Rakociński, M., Racki, G., Bond, D. P., Sobień, K., & Claeys, P. (2013). The astronomical rhythm of Late-Devonian climate change (Kowala section, Holy Cross Mountains, Poland). *Earth and Planetary Science Letters*, *365*, 25–37. https://doi.org/10.1016/j.epsl.2013.01.016

Dietz, C., & Fuchs, A. (1935). *Erläuterungen zur Geologischen Karte von Preussen und benachbarten Bundesstaaten: Blatt 4910 Lindlar*. Preußische Geologische Landesanstalt.

Dyson, I. A. (1996). Significance of hummocky cross-stratification and quasi-planar lamination in the lower Devonian Walhalla group at Cape Liptrap, Victoria. *Australian Journal of Earth Sciences*, *43*(2), 189–199. https://doi.org/10.1080/08120099608728247

Ebert, A., & Müller, H. (1973). *Erläuterungen zu Blatt 4715 Eslohe*. Geologisches Landesamt Nordrhein-Westfalen.

Eilertsen, R. S., Corner, G. D., Aasheim, O. D., & Hansen, L. (2011). Facies characteristics and architecture related to palaeodepth of Holocene fjord-delta sediments. *Sedimentology*, *58*(7), 1784–1809. https://doi.org/10.1111/j.1365-3091.2011.01239.x

Engel, W., Franke, W., & Langenstrassen, F. (1983). Palaeozoic Sedimentation in the Northern Branch of the Mid-European Variscides — Essay of an Interpretation. In H. Martin & F. W. Eder (Eds.), *Intracontinental Fold Belts: Case Studies in the Variscan Belt of Europe and the Damara Belt in Namibia* (pp. 9–41). Springer Berlin Heidelberg. https://doi.org/10.1007/978-3-642-69124-9_2

Feng, W.-J., Zhang, C.-M., Yin, T.-J., Yin, Y.-S., Liu, J.-L., Zhu, R., Xu, Q.-H., & Chen, Z. (2019). Sedimentary characteristics and internal architecture of a river-dominated delta controlled by autogenic process: implications from a flume tank experiment. *Petroleum Science*, *16*(6), 1237–1254. https://doi.org/10.1007/s12182-019-00389-x

Flemming, B. W., Schubert, H., Hertweck, G., & Müller, K. (1992). Bioclastic Tidal-Channel Lag Deposits: a Genetic Model. *Senckenbergiana Maritima*, *22*(3), 106–129.

Folk, R. L. (1974). *Petrology of Sedimentary Rocks*. Hemphill Pub. Co.

Franke, W. (2024). The Rheic riddle: ocean closed, but no orogen. *Geological Society, London, Special Publications*, *542*(1), Article SP542-2022-354. https://doi.org/10.1144/SP542-2022-354

Fuchs, A. (1919). Über einige Fälle von örtlichem Facieswechsel im sauerländischen Faciesgebiet. *Jahrbuch Der Preussischen Geologischen Landesanstalt Zu Berlin*, *40*, XXI–XXXI.

Fuchs, A. (1922). *Erläuterungen zur Geologischen Karte von Preussen und benachbarten Bundesstaaten: Blatt 4812 Herscheid*. Preußische Geologische Landesanstalt.

Fuchs, A. (1923). *Erläuterungen zur Geologischen Karte von Preussen und benachbarten Bundesstaaten: Blatt 4712 Altena*. Preußische Geologische Landesanstalt.

Fuchs, A., & Schmidt, W. E. (1928). *Erläuterungen zur Geologischen Karte von Preussen und benachbarten Bundesstaaten: Blatt 4911 Gummersbach*. Preußische Geologische Landesanstalt.

García-García, F., Corbí, H., Soria, J. M., & Viseras, C. (2011). Architecture analysis of a river flood-dominated delta during an overall sea-level rise (early Pliocene, SE Spain). *Sedimentary Geology*, *237*(1-2), 102–113. https://doi.org/10.1016/j.sedgeo.2011.02.010

Gosny, O. (2010). Conchostraken und leperditicopide Ostracoden aus der mitteldevonischen Brandenberg-Formation des Bergischen Landes. *Decheniana*, *163*, 159–167. https://doi.org/10.21248/decheniana.v163.4640

Grabert, H. (1969). *Erläuterungen zu Blatt 4912 Drolshagen*. Geologisches Landesamt Nordrhein-Westfalen.

Grabert, H. (1970). *Erläuterungen zu Blatt 5011 Wiehl*. Geologisches Landesamt Nordrhein-Westfalen.

Grabert, H. (1971). Der Steinbruch von Unnenberg bei Gummersbach. *Sauerländischer Gebirgsbote: Zeitschrift Des Sauerländischen Gebirgsvereins Für Wandern Und Heimat, Landespflege Und Fremdenverkehr*, *73*, 5–7.

Grundvåg, S.-A., Helland-Hansen, W., Johannessen, E. P., Eggenhuisen, J., Pohl, F., & Spychala, Y. (2023). Deep-water sand transfer by hyperpycnal flows, the Eocene of Spitsbergen, Arctic Norway. *Sedimentology*, Article sed.13105. Advance online publication. https://doi.org/10.1111/sed.13105

Grundvåg, S.-A., Jelby, M. E., Olaussen, S., & Śliwińska, K. K. (2021). The role of shelf morphology on storm-bed variability and stratigraphic architecture, Lower Cretaceous, Svalbard. *Sedimentology*, *68*(1), 196–237. https://doi.org/10.1111/sed.12791

Heerema, C. J., Talling, P. J., Cartigny, M. J. B., Paull, C. K., Bailey, L., Simmons, S. M., Parsons, D. R., Clare, M. A., Gwiazda, R., Lundsten, E., Anderson, K., Maier, K. L., Xu, J. P., Sumner, E. J., Rosenberger, K., Gales, J., McGann, M., Carter, L., & Pope, E. L. (2020). What determines the downstream evolution of turbidity currents? *Earth and Planetary Science Letters*, *532*, 116023. https://doi.org/10.1016/j.epsl.2019.116023

Henkel, D. J. (1970). The Role of Waves in Causing Submarine Landslides. *Géotechnique*, *20*(1), 75–80. https://doi.org/10.1680/geot.1970.20.1.75

Hepp, D. A., Romero, O. E., Mörz, T., de Pol-Holz, R., & Hebbeln, D. (2019). How a river submerges into the sea: a geological record of changing a fluvial to a marine paleoenvironment during early Holocene sea level rise. *Journal of Quaternary Science*, *34*(7), 581–592. https://doi.org/10.1002/jqs.3147

Hesse, R., & Khodabakhsh, S. (1998). Depositional facies of late Pleistocene Heinrich events in the Labrador Sea. *Geology*, *26*(2), 103. https://doi.org/10.1130/0091-7613(1998)026<0103:DFOLPH>2.3.CO;2

Horn, B. L. D., Goldberg, K., & Schultz, C. L. (2018). Interpretation of massive sandstones in ephemeral fluvial settings: A case study from the Upper Candelária Sequence (Upper Triassic, Paraná Basin, Brazil). *Journal of South American Earth Sciences*, *81*, 108–121. https://doi.org/10.1016/j.jsames.2017.10.009

Hoyal, D., van Wagoner, J. C., Adair, N. L., Deffenbaugh, M., Li, D., Sun, C., Huh, C.-A., & Griffin, D. E. (2003). *Sedimentation from Jets: A Depositional Model for Clastic Deposits of all Scales and Environments*. AAPG Annual Meeting, May 14, 2003, Salt Lake City, Utah.

Hüneke, H., & Mulder, T. (2011). *Deep-Sea Sediments*. *Developments in Sedimentology: Vol. 63*. Elsevier Science & Technology. https://ebookcentral.proquest.com/lib/kxp/detail.action?docID=629936

Hunter, R. E. (1977). Terminology of Cross-Stratified Sedimentary Layers and Climbing-Ripple Structures. *Journal of Sedimentary Research*, *Vol. 47.* https://doi.org/10.1306/212F7225-2B24-11D7-8648000102C1865D

Irastorza, A., Zavala, C., Campetella, D. M., Turienzo, M., Olivera, D., Peralta, F., Irastorza, M., & Martz, P. (2021). Hyperpycnal littoral deltas: A case of study from the Lower Cretaceous Agrio Formation in the Neuquén Basin, Argentina. *Journal of Palaeogeography*, *10*(4), 550–570. https://doi.org/10.1016/j.jop.2021.11.004

Jansen, U. (2016). Brachiopod faunas, facies and biostratigraphy of the Pridolian to lower Eifelian succession in the Rhenish Massif (Rheinisches Schiefergebirge, Germany). *Geological Society, London, Special Publications*, *423*(1), 45–122. https://doi.org/10.1144/SP423.11

Jelby, M. E., Grundvåg, S.-A., Helland-Hansen, W., Olaussen, S., & Stemmerik, L. (2020). Tempestite facies variability and storm-depositional processes across a wide ramp: Towards a polygenetic model for hummocky cross-stratification. *Sedimentology*, *67*(2), 742–781. https://doi.org/10.1111/sed.12671

Johnson, J. G., Klapper, G., & Sandberg, C. A. (1985). Devonian eustatic fluctuations in Euramerica. *Geological Society of America Bulletin*, *96*(5), 567–587. https://doi.org/10.1130/0016-7606(1985)96<567:DEFIE>2.0.CO;2

Jux, U. (1960). Die devonischen Riffe im Rheinischen Schiefergebirge: Teil I. *Neues Jahrbuch Für Geologie Und Paläontologie, Abhandlungen*, *110*(2), 186–258.

Jux, U. (1983). *Erläuterungen zu Blatt 5010 Engelskirchen*. Geologisches Landesamt Nordrhein-Westfalen.

Kaufmann, B. (2006). Calibrating the Devonian Time Scale: A synthesis of U–Pb ID–TIMS ages and conodont stratigraphy. *Earth-Science Reviews*, *76*(3-4), 175–190. https://doi.org/10.1016/j.earscirev.2006.01.001

Kerr, M., & Eyles, N. (1991). Storm-deposited sandstones (tempestites) and related ichnofossils of the Late Ordovician Georgian Bay Formation, southern Ontario, Canada. *Canadian Journal of Earth Sciences*, *28*(2), 266–282. https://doi.org/10.1139/e91-026

Klitzsch, E. (1959). Das Mitteldevon am Nordwestrand der Dillmulde. *Zeitschrift Der Deutschen Geologischen Gesellschaft*, *111*, 366–409.

Kneller, B., & Buckee, C. (2000). The structure and fluid mechanics of turbidity currents: a review of some recent studies and their geological implications. *Sedimentology*, *47*, 62–94. https://doi.org/10.1046/j.1365-3091.2000.047s1062.x

Koch, L. (2023). Fossilien aus dem GeoPark Ruhrgebiet: Einige ausgewählte Pflanzenfossilien aus dem Unteren Mitteldevon von Hagen-Ambrock. *GeoPark Ruhrgebiet News*, *31*(1), 10–12.

Kondo, Y., Abbott, S. T., Kitamura, A., Kamp, P. J., Naish, T. R., Kamataki, T., & Saul, G. S. (1998). The relationship between shellbed type and sequence architecture: examples from Japan and

New Zealand. *Sedimentary Geology*, *122*(1-4), 109–127. https://doi.org/10.1016/S0037-0738(98)00101-8

Königshof, P., Becker, R. T, & Hartenfels S. (2016). The Rhenish Massif as a part of the European Variscides. *Münstersche Forschungen Zur Geologie Und Palaeontologie*, *108*, 1–13.

Königshof, P., Nesbor, H.-D., & Flick, H. (2010). Volcanism and reef development in the Devonian: A case study from the Lahn syncline, Rheinisches Schiefergebirge (Germany). *Gondwana Research*, *17*(2-3), 264–280. https://doi.org/10.1016/j.gr.2009.09.006

Krebs, W. (1979). Devonian Basinal Facies. *Special Papers in Palaeontology*, *23*, 125–139.

Kuehl, S. A., DeMaster, D. J., & Nittrouer, C. A. (1986). Nature of sediment accumulation on the Amazon continental shelf. *Continental Shelf Research*, *6*(1-2), 209–225. https://doi.org/10.1016/0278-4343(86)90061-0

Kuenen, P. H., & Humbert, F. L. (1969). Grain Size of Turbidite Ripples. *Sedimentology*, *13*(3-4), 253–261. https://doi.org/10.1111/j.1365-3091.1969.tb00172.x

Kvale, E. P., Archer, A. W., & Johnson, H. R. (1989). Daily, monthly, and yearly tidal cycles within laminated siltstones of the Mansfield Formation (Pennsylvanian) of Indiana. *Geology*, *17*(4), 365. https://doi.org/10.1130/0091-7613(1989)017<0365:DMAYTC>2.3.CO;2

Lamb, M. P., Myrow, P. M., Lukens, C., Houck, K., & Strauss, J. (2008). Deposits from Wave-Influenced Turbidity Currents: Pennsylvanian Minturn Formation, Colorado, U.S.A. *Journal of Sedimentary Research*, *78*(7), 480–498. https://doi.org/10.2110/jsr.2008.052

Langenstrassen, F. (1972). Fazies und Stratigraphie der Eifel-Stufe im östlichen Sauerland (Rheinsiches Schiefergebirge, Bl. Schmallenberg und Girkhausen). *Göttinger Arbeiten Zur Geologie Und Paläontologie*, *12*.

Langenstrassen, F. (1982). Sedimentologie und biofazielle Untersuchungen an Proben aus der Bohrung Schwarzbachtal 1 (Rheinisches Schiefergebirge, Velberter Sattel). *Senckenbergiana Lethaea*, *63*(1/4), 315–333.

Langenstrassen, F. (1983). Neritic Sedimentation of the Lower and Middle Devonian in the Rheinische Schiefergebirge East of the River Rhine. In H. Martin & F. W. Eder (Eds.), *Intracontinental Fold Belts: Case Studies in the Variscan Belt of Europe and the Damara Belt in Namibia* (pp. 43–76). Springer Berlin Heidelberg. https://doi.org/10.1007/978-3-642-69124-9_3

Langenstrassen, F., Becker, G., & Gross-Uffenorde, H. (1979). Zur Fazies und Fauna der Brandenberg-Schichten bei Lasbeck (Eifel-Stufe, Rechtsrheinisches Schiefergebirge). *Neues Jahrbuch Für Geologie Und Paläontologie, Abhandlungen*, *158*, 64–99.

Lin, W., & Bhattacharya, J. P. (2021). Storm-flood-dominated delta: A new type of delta in stormy oceans. *Sedimentology*, *68*(3), 1109–1136. https://doi.org/10.1111/sed.12819

Lippert, H.-J., Hentschel, H., & Rabien, A. (1970). *Erläuterungen zur Geologischen Karte von Hessen: Blatt 5215 Dillenburg: 2. neu bearbeitete Auflage*. Hessisches Landesamt für Bodenforschung.

Longhitano, S. G., Sabato, L., Tropeano, M., & Gallicchio, S. (2010). A Mixed Bioclastic-Siliciclastic Flood-Tidal Delta in a Micro Tidal Setting: Depositional Architectures and Hierarchical Internal Organization (Pliocene, Southern Apennine, Italy). *Journal of Sedimentary Research*, *80*(1), 36–53. https://doi.org/10.2110/jsr.2010.004

Luo, K., Su, M., Liu, S., Shi, J., Wang, C., Chen, H., Yang, S., Lin, Z., & Wei, L. (2023). Sea-level, climate, and oceanographic controls on recent deepwater hyperpycnites: A case example from the shenhu slope (northern South China Sea). *Quaternary Science Reviews*, *311*, 108148. https://doi.org/10.1016/j.quascirev.2023.108148

Marshall, J., & Fletcher, T. P. (2002). Middle Devonian (Eifelian) spores from a fluvial dominated lake margin in the Orcadian Basin, Scotland. *Review of Palaeobotany and Palynology*, *118*(1-4), 195–209. https://doi.org/10.1016/S0034-6667(01)00114-2

Mehrtens, C. J. (1988). Bioclastic Turbidites in the Trenton Limestone. In B. D. Keith (Ed.), *The Trenton Group (Upper Ordovician Series) of Eastern North America* (pp. 87–112). American Association of Petroleum Geologists. https://doi.org/10.1306/St29491C7

Meischner, D. (1971). Clastic sedimentation in the Variscan Geosyncline east of the river Rhine. In G. Müller (Ed.), *Sedimentology of parts of Central Europe: Guidebook to excursions held during the VIII International Sedimentological Congress 1971 in Heidelberg, Germany* (pp. 9–43). Kramer.

Meyer, K. (1981). *Geochemische Untersuchungen an Spiliten, Pikriten, Quarzkeratophyren and Keratophyren des Rhenoherzynikums* [Dissertation]. Georg-August-Universität zu Göttingen.

Michael J. Soreghan, A. S. (1996). Textural and compositional variability across littoral segments of Lake Tanganyika: The effect of asymmetric basin structure on sedimentation in large rift lakes. *AAPG Bulletin*, *80.* https://doi.org/10.1306/64ED87F0-1724-11D7-8645000102C1865D

Middleton, G. V. (1967). The orientation of concavo-convex particles deposited from experimental turbidity currents. *Journal of Sedimentary Research*, *37*(1), 229–232. https://doi.org/10.1306/74D716A4-2B21-11D7-8648000102C1865D

Mohseni, H., & Al-Aasm, I. S. (2004). Tempestite deposits on a storm-influenced carbonate ramp: an example from the Pabdeh formation (Paleogene), Zagros Basin, SW Iran. *Journal of Petroleum Geology*, *27*(2), 163–178. https://doi.org/10.1111/j.1747-5457.2004.tb00051.x

Molina, J. M., Alfaro, P., Moretti, M. & Soria, J. M. (1998). Soft-sediment deformation structures induced by cyclic stress of storm waves in tempestites (Miocene, Guadalquivir Basin, Spain). *Terra Nova*, *10*(3), 145–150. https://doi.org/10.1046/j.1365-3121.1998.00183.x

Molina, J. M., Ruiz-Ortiz, P. A., & Vera, J. A. (1997). Calcareous tempestites in pelagic facies (Jurassic, Betic Cordilleras, Southern Spain). *Sedimentary Geology*, *109*(1-2), 95–109. https://doi.org/10.1016/S0037-0738(96)00057-7

Mulder, T, & Alexander, J. (2001). The physical character of subaqueous sedimentary density flows and their deposits. *Sedimentology*, *48*(2), 269–299. https://doi.org/10.1046/j.1365-3091.2001.00360.x

Mulder, T, Syvitski, J. P., Migeon, S., Faugères, J.-C., & Savoye, B. (2003). Marine hyperpycnal flows: initiation, behavior and related deposits. A review. *Marine and Petroleum Geology*, *20*(6-8), 861–882. https://doi.org/10.1016/j.marpetgeo.2003.01.003

Mustafa, H. (1975). Beiträge zur Devonflora I. *Argumenta Palaeobotanica*, *4*, 101–133.

Mustafa, H. (1978a). Beiträge zur Devonflora II. *Argumenta Palaeobotanica*, *5*, 31–56.

Mustafa, H. (1978b). Beiträge zur Devonflora III. *Argumenta Palaeobotanica*, *5*, 91–132.

Mutti, E., Tinterri, R., Benevelli, G., Di Biase, D., & Cavanna, G. (2003). Deltaic, mixed and turbidite sedimentation of ancient foreland basins. *Marine and Petroleum Geology*, *20*(6-8), 733–755. https://doi.org/10.1016/j.marpetgeo.2003.09.001

Mutti, E., Tinterri, R., Di Biase, D., Fava, L., Mavilla, N., Angella, S., & Calabrese, L. (2000). Delta-front facies associations of ancient flood-dominated fluvio-deltaic systems. *Revista De La Sociedad Geológica De España*, *13*(2), 165–190.

Myrow, P. M. (2005). SEDIMENTARY ENVIRONMENTS | Storms and Storm Deposits. In *Encyclopedia of Geology* (pp. 580–587). Elsevier. https://doi.org/10.1016/B0-12-369396-9/00488-3

Nesbor, H.-D. (2004). Paläozoischer Intraplattenvulkanismus im östlichen Rheinischen Schiefergebirge – Magmenentwicklung und zeitlicher Ablauf. *Geologisches Jahrbuch Hessen*, *131*, 145–182.

Olariu, M. I. (2023). Sedimentology and stratigraphy of the earliest deltaic shorelines of the Paleocene Lower Wilcox Group in the Gulf of Mexico. *Journal of Sedimentary Research*, *93*(8), 522–540. https://doi.org/10.2110/jsr.2021.084

Onorato, M. R., Perucca, L., Coronato, A., Rabassa, J., & López, R. (2016). Seismically-induced soft-sediment deformation structures associated with the Magallanes–Fagnano Fault System (Isla Grande de Tierra del Fuego, Argentina). *Sedimentary Geology*, *344*, 135–144. https://doi.org/10.1016/j.sedgeo.2016.04.010

Otto, M. (1999). New finds of vertebrates in the Middle Devonian Brandenberg Group (Sauerland, Northwest Germany). *Paläontologische Zeitschrift*, *73*(1-2), 113–131. https://doi.org/10.1007/BF02987986

Overeem, I., Kroonenberg, S. B., Veldkamp, A., Groenesteijn, K., Rusakov, G. V., & Svitoch, A. A. (2003). Small-scale stratigraphy in a large ramp delta: recent and Holocene sedimentation in the Volga delta, Caspian Sea. *Sedimentary Geology*, *159*(3-4), 133–157. https://doi.org/10.1016/S0037-0738(02)00256-7

Owen, G. (1987). Deformation processes in unconsolidated sands. *Geological Society, London, Special Publications*, *29*(1), 11–24. https://doi.org/10.1144/GSL.SP.1987.029.01.02

Owen, G., & Moretti, M. (2011). Identifying triggers for liquefaction-induced soft-sediment deformation in sands. *Sedimentary Geology*, *235*(3-4), 141–147. https://doi.org/10.1016/j.sedgeo.2010.10.003

Pattison, S. A. J. (2005). Storm-Influenced Prodelta Turbidite Complex in the Lower Kenilworth Member at Hatch Mesa, Book Cliffs, Utah, U.S.A.: Implications for Shallow Marine Facies Models. *Journal of Sedimentary Research*, *75*(3), 420–439. https://doi.org/10.2110/jsr.2005.033

Peng, Y., Steel, R. J., & Olariu, C. (2017). Transition from storm wave-dominated outer shelf to gullied upper slope: The mid-Pliocene Orinoco shelf margin, South Trinidad. *Sedimentology*, *64*(6), 1511–1539. https://doi.org/10.1111/sed.12362

Pfeiffer, A. (1938). *Die Brandenbergschichten im bergisch-sauerländischen Mitteldevon* [Dissertation]. Georg-August-Universität zu Göttingen.

Plessmann, W., & Spaeth, G. (1971). Sedimentgänge und tektonisches Schichtfließen (Biegungsfließen) im Rechtsrheinischen Schiefergebirge. *Geologische Mitteilungen*, *11*, 137–164.

Plink-Björklund, P. (2015). Morphodynamics of rivers strongly affected by monsoon precipitation: Review of depositional style and forcing factors. *Sedimentary Geology*, *323*, 110–147. https://doi.org/10.1016/j.sedgeo.2015.04.004

Ponciano, L. C. M. d. O., Da Fonseca, V. M. M., & Da Machado, D. M. C. (2012). Taphofacies analysis of late early Givetian fossil assemblages of the Parnaíba Basin (State of Piauí, northeast Brazil). *Palaeogeography, Palaeoclimatology, Palaeoecology*, *326-328*, 95–108. https://doi.org/10.1016/j.palaeo.2012.02.008

Ponciano, L. C. M. d. O., & Della Fávera, J. C. (2009). Flood-dominated fluvio-deltaic system: a new depositional model for the Devonian Cabeças Formation, Parnaíba Basin, Piauí, Brazil. *Anais Da Academia Brasileira De Ciências*, *81*(4), 769–780. https://doi.org/10.1590/S0001-37652009000400014

Reuter, A. (1993). Analyse eines regradierenden Deltas im Mittel-Devon des Rheinischen Schiefergebirges. *Göttinger Arbeiten Zur Geologie Und Paläontologie*, *57*.

Ribbert, K.-H. (1998a). Attendorn-Elsper Doppelmulde; Mitteldevon. In K. Weddige (Ed.), *Senckenbergiana lethaea: 77(1/2). Devon-Korrelationstabelle* (312, column R014dm97).

Ribbert, K.-H. (1998b). Briloner Sattel (Nordrand), Ostsauerländer Hauptsattel (Ostteil); Mitteldevon. In K. Weddige (Ed.), *Senckenbergiana lethaea: 77(1/2). Devon-Korrelationstabelle* (311, column R010dm97).

Ribbert, K.-H. (1998c). Gummersbacher Mulde, Ebbe Sattel; Mitteldevon. In K. Weddige (Ed.), *Senckenbergiana lethaea: 77(1/2). Devon-Korrelationstabelle* (312, column R013dm97).

Ribbert, K.-H. (1998d). Latroper Sattel (SE-Flanke); Mitteldevon. In K. Weddige (Ed.), *Senckenbergiana lethaea: 77(1/2). Devon-Korrelationstabelle* (313, column R017dm97).

Ribbert, K.-H. (1998e). Ostsauerländer Hauptsattel, Latroper Sattel; Mitteldevon. In K. Weddige (Ed.), *Senckenbergiana lethaea: 77(1/2). Devon-Korrelationstabelle* (313, column R016dm97).

Ribbert, K.-H. (1998f). Paffrather Mulde, Bergische Muldenzone; Mitteldevon. In K. Weddige (Ed.), *Senckenbergiana lethaea: 77(1/2). Devon-Korrelationstabelle* (312, column R012dm97).

Ribbert, K.-H. (1998g). Paffrather Mulde, Remscheid-Altenaer Sattel; Mitteldevon. In K. Weddige (Ed.), *Senckenbergiana lethaea: 77(1/2). Devon-Korrelationstabelle* (311, column R011dm97).

Ribbert, K.-H. (1998h). Remscheid-Altenaer Sattel (Mittlerer Teil); Mitteldevon. In K. Weddige (Ed.), *Senckenbergiana lethaea: 77(1/2). Devon-Korrelationstabelle* (310, column R007dm97).

Ribbert, K.-H. (1998i). Remscheid-Altenaer Sattel (Ostteil) und Lüdenscheider Mulde; Mitteldevon. In K. Weddige (Ed.), *Senckenbergiana lethaea: 77(1/2). Devon-Korrelationstabelle* (310, column R008dm97).

Ribbert, K.-H. (1998j). Remscheid-Altenaer Sattel (Westteil); Mitteldevon. In K. Weddige (Ed.), *Senckenbergiana lethaea: 77(1/2). Devon-Korrelationstabelle* (310, column R006dm97).

Ribbert, K.-H. (1998k). Warsteiner Sattel (Nordrand), Ostsauerländer Hauptsattel (Westteil); Mitteldevon. In K. Weddige (Ed.), *Senckenbergiana lethaea: 77(1/2). Devon-Korrelationstabelle* (311, column R009dm97).

Ribbert, K.-H. (2013). *Erläuterungen zu Blatt 4911 Gummersbach: 2., neu bearbeitete Auflage*. Geologischer Dienst Nordrhein-Westfalen.

Ribbert, K.-H., & Baumgarten, H. (2012). *Geologie im Rheinischen Schiefergebirge - Teil 2: Bergisches Land*. *Geologie im Rheinischen Schiefergebirge: / Geologischer Dienst NRW ; Teil 2*. Geologischer Dienst NRW.

Ribbert, K.-H., Wrede, V., Oesterreich, B., Baumgarten, H., Gawlik, A., & Heuser, H. (2017). *Geologie im Rheinischen Schiefergebirge - Teil 3: Sauer- und Siegerland*. *Geologie im Rheinischen Schiefergebirge: / Geologischer Dienst NRW ; Teil 3*. Geologischer Dienst Nordrhein-Westfalen.

Rodríguez-Tovar, F. J. (2022). Ichnological analysis: A tool to characterize deep-marine processes and sediments. *Earth-Science Reviews*, *228*, 104014. https://doi.org/10.1016/j.earscirev.2022.104014

Safak, I., Allison, M. A., & Sheremet, A. (2013). Floc variability under changing turbulent stresses and sediment availability on a wave energetic muddy shelf. *Continental Shelf Research*, *53*, 1–10. https://doi.org/10.1016/j.csr.2012.11.015

Saller, A., Lin, R., & Dunham, J. (2006). Leaves in turbidite sands: The main source of oil and gas in the deep-water Kutei Basin, Indonesia. *AAPG Bulletin*, *90*(10), 1585–1608. https://doi.org/10.1306/04110605127

Schaumann, R. M., Capperucci, R. M., Bungenstock, F., McCann, T., Enters, D., Wehrmann, A., & Bartholomä, A. (2021). The Middle Pleistocene to early Holocene subsurface geology of the Norderney tidal basin: new insights from core data and high-resolution sub-bottom profiling (Central Wadden Sea, southern North Sea). *Netherlands Journal of Geosciences*, *100*, E15. https://doi.org/10.1017/njg.2021.3

Scheffler, S. M., Da Silva, C. F., Fernandes, A. C. S., & Da Fonseca, V. M. M. (2010). Crinóides da borda leste da bacia do Parnaíba (Formação Cabeças, Devoniano Médio). *Boletim Do Museu Paraense Emílio Goeldi - Ciências Naturais*, *5*(2), 165–173. https://doi.org/10.46357/bcnaturais.v5i2.640

Schnapperelle, S., Kachelgrieß, G., Kühn, R., Methner, S., Schulz, C., & Mertmann, D. (2021). Devonischer Vulkanismus und Sedimentation im Gebiet Padberg und Giershagen, NE Rheinisches Schiefergebirge. *Hallesches Jahrbuch Für Geowissenschaften*, *44*, 7–43.

Schultze, L. K. P., Merckelbach, L. M., & Carpenter, J. R. (2020). Storm-induced turbulence alters shelf sea vertical fluxes. *Limnology and Oceanography Letters*, *5*(3), 264–270. https://doi.org/10.1002/lol2.10139

Schweitzer, H.-J. (1990). Pflanzen erobern das Land. *Kleine Senckenberg-Reihe*, *18*, 1–75.

Scotese, C. R. (2016). *PALEOMAP PaleoAtlas for GPlates and the PaleoData Plotter Program, PALEOMAP Project*. https://www.earthbyte.org/paleomap-paleoatlas-for-gplates/

Shanmugam, G. (2018). The hyperpycnite problem. *Journal of Palaeogeography*, *7*(1). https://doi.org/10.1186/s42501-018-0001-7

Shanmugam, G. (2019). Reply to discussions by Zavala (2019) and by Van Loon, Hüeneke, and Mulder (2019) on Shanmugam, G. (2018, Journal of Palaeogeography, 7 (3): 197–238): 'the hyperpycnite problem'. *Journal of Palaeogeography*, *8*(1). https://doi.org/10.1186/s42501-019-0047-1

Simons, D. B., Richardson, E. V., & Nordin, C. F. (1965). Sedimentary structures generated by flow on alluvial channels. In G. V. Middleton (Ed.), *SEPM Special Publication. Primary sedimentary structures and their hydrodynamic interpretation* (Vol. 12, pp. 34–52). SEPM Special Publication.

Sparks, R. S. J., Bonnecaze, R. T., Huppert, H. E., Lister, J. R., Hallworth, M. A., Mader, H., & Phillips, J. (1993). Sediment-laden gravity currents with reversing buoyancy. *Earth and Planetary Science Letters*, *114*(2-3), 243–257. https://doi.org/10.1016/0012-821X(93)90028-8

Spriestersbach, J. (1942). Lenneschiefer: Stratigraphie, Fazies und Fauna. *Abhandlungen Des Reichsamts Für Bodenforschung / Neue Folge*, *203*. https://books.google.de/books?id=9C8RAAAAIAAJ

Stanley, K. O. (1974). Morphology and Hydraulic Significance of Climbing Ripples with Superimposed Micro-Ripple-Drift Cross-lamination in Lower Quaternary Lake Silts, Nebraska. *Journal of Sedimentary Research*, *44*, 472-283. https://doi.org/10.1306/74D72A63-2B21-11D7-8648000102C1865D

Steel, E., Simms, A. R., Steel, R. J., & Olariu, C. (2018). Hyperpycnal delivery of sand to the continental shelf: Insights from the Jurassic Lajas Formation, Neuquén Basin, Argentina. *Sedimentology*, *65*(6), 2149–2170. https://doi.org/10.1111/sed.12460

Steel, E., Simms, A. R., Warrick, J., & Yokoyama, Y. (2016). Highstand shelf fans: The role of buoyancy reversal in the deposition of a new type of shelf sand body. *Geological Society of America Bulletin*, *128*(11-12), 1717–1724. https://doi.org/10.1130/B31438.1

Stets, J., & Schäfer, A. (2002). Depositional environments in the lower Devonian siliciclastics of the Rhenohercynian Basin (Rheinisches Schiefergebirge, W-Germany). *Contributions to Sedimentary Geology*, *22*.

Stow, D. A. V., & Wetzel, A. (1990). Hemiturbidite: A New Type of Deep-Water Sediment. In J. R. Cochran & D. A. V. Stow (Eds.), *Proceedings of the Ocean Drilling Program. Proceedings of the Ocean Drilling Program, 116 Scientific Results* (Vol. 116). Ocean Drilling Program. https://doi.org/10.2973/odp.proc.sr.116.152.1990

Streel, M. (2000). Late Frasnian–Famennian climates based on palynomorph analyses and the question of the Late Devonian glaciations. *Earth-Science Reviews*, *52*(1-3), 121–173. https://doi.org/10.1016/S0012-8252(00)00026-X

Sumner, E. J., Amy, L. A., & Talling, P. J. (2008). Deposit Structure and Processes of Sand Deposition from Decelerating Sediment Suspensions. *Journal of Sedimentary Research*, *78*(8), 529–547. https://doi.org/10.2110/jsr.2008.062

Suttner, T. J., Kido, E., Joachimski, M. M., Vodrážková, S., Pondrelli, M., Corradini, C., Corriga, M. G., Simonetto, L., & Kubajko, M. (2021). Paleotemperature record of the Middle Devonian Kačák Episode. *Scientific Reports*, *11*(1), 16559. https://doi.org/10.1038/s41598-021-96013-3

Tanner, W. F. (1968). Environmental Indicators in Morrison Formation, New Mexico: ABSTRACT. *AAPG Bulletin*, *52*, 522. https://doi.org/10.1306/5D25C3CB-16C1-11D7-8645000102C1865D

Tavares Calandrini de Azevedo, J. V., Batista, Z. V., Ferreira de Lima Filho, M., Oliveira Agostinho, S. M., Neto, E. F., Lima de Moura, W. A., & Rodrigues Barbosa Van, T. W. (2024). Facies analysis and paleoenvironment of the Poti formation in the ITAUEIRA and FLORIANO region: Contribution to the Carboniferous depositional history of the Parnaíba basin. *Journal of South American Earth Sciences*, 104806. https://doi.org/10.1016/j.jsames.2024.104806

Thienhaus, R. (1940). Die Faziesverhältnisse im Südwestteil der Attendorner Mulde und ihre Bedeutung für die Stratigraphie des bergisch-sauerländischen Mitteldevons. *Abhandlungen Des Reichsamts Für Bodenforschung*, *199*.

Thünker, M. (2011). *Erläuterungen zu Blatt 4913 Olpe: 2., völlig neu bearbeitete Auflage*. Geologischer Dienst Nordrhein-Westfalen.

Tinterri, R. (2011). Combined flow sedimentary structures and the genetic link between sigmoidal- and hummocky-cross stratification, *10*, 43–85.

van Loon, A. J., Hüneke, H., & Mulder, T. (2019). The hyperpycnite problem: comment. *Journal of Palaeogeography*, *8*(1). https://doi.org/10.1186/s42501-019-0034-6

van Wagoner, J. C., Mitchum, R. M., Campion, K. M., & v. d. Rahmanian. (1996). *Siliciclastic sequence stratigraphy in well logs, cores, and outcrops: Concepts for high-resolution correlation of time and facies* (4. print). *AAPG methods in exploration series: Vol. 7*. AAPG.

van Wagoner, J. C., Posamentier, H. W., Mitchum, R. M., Vail, P. R., Sarg, J. F., Loutit, T. S., & Hardenbol, J. (1988). An Overview of the Fundamentals of Sequence Stratigraphy and Key Definitions. In C. K. Wilgus, B. S. Hastings, H. Posamentier, J. van Wagoner, C. A. Ross, & C. G. C. St. Kendall (Eds.), *Sea-Level Changes* (pp. 39–45). SEPM (Society for Sedimentary Geology). https://doi.org/10.2110/pec.88.01.0039

Visser, M. J. (1980). Neap-spring cycles reflected in Holocene subtidal large-scale bedform deposits: A preliminary note. *Geology*, *8*(11), 543. https://doi.org/10.1130/0091-7613(1980)8<543:NCRIHS>2.0.CO;2

von Kamp, H., Ribbert, K.-H., & Clausen, C.-D. (2017). *Erläuterungen zu Blatt C 5110 Gummersbach: 2., überarbeitete und aktualisierte Auflage*. *Geologische Karte von Nordrhein-Westfalen / Geologisches Landesamt Nordrhein-Westfalen: Erläuterungen C 5110*. Geologisches Landesamt Nordrhein-Westfalen.

Wang, H., Bi, N., Wang, Y., Saito, Y., & Yang, Z. (2010). Tide-modulated hyperpycnal flows off the Huanghe (Yellow River) mouth, China. *Earth Surface Processes and Landforms*, *35*(11), 1315–1329. https://doi.org/10.1002/esp.2032

Weddige, K. (1977). Die Conodonten der Eifel-Stufe im Typusgebiet und in benachbarten Faziesgebieten. *Senckenbergiana Lethaea*, *58*, 271–419.

Werner, W. (1988). Synsedimentary Faulting and Sediment-Hosted Submarine Hydrothermaal Mineralization: A Case Study in the Rhenish Massif, Germany. *Göttinger Arbeiten Zur Geologie Und Paläontologie*, *36*.

Wilson, R. D., & Schieber, J. (2014). Muddy Prodeltaic Hyperpycnites In the Lower Genesee Group of Central New York, USA: Implications For Mud Transport In Epicontinental Seas. *Journal of Sedimentary Research*, *84*(10), 866–874. https://doi.org/10.2110/jsr.2014.70

Wing, S. L. (1984). Relation of Paleovegetation to Geometry and Cyclicity of Some Fluvial Carbonaceous Deposits. *Journal of Sedimentary Research*, *54*(1), 52–66. https://doi.org/10.1306/212F83A0-2B24-11D7-8648000102C1865D

Witzke, B. J., & Heckel, P. H. (1988). Paleoclimatic indicators and inferred Devonian paleolatitudes of Euramerica. In N. J. McMillan, A. F. Embry, & D. J. Glass (Eds.), *Canadian Society of Petroleum Geologists Memoirs. Devonian of the World* (pp. 49–63).

Worm, H.-U., Ahmed, A. M. M., Ahmed, N. U., Islam, H. O., Huq, M. M., Hambach, U., & Lietz, J. (1998). Large sedimentation rate in the Bengal delta: Magnetostratigraphic dating of Cenozoic sediments from northeastern Bangladesh. *Geology*, *26*(6), 487. https://doi.org/10.1130/0091-7613(1998)026%3C0487:LSRITB%3E2.3.CO;2

Yamaguchi, N., & Sekiguchi, H. (2010). Effects of Settling and Preferential Deposition of Sediment on Ripple Roundness Under Shoaling Waves. *Journal of Sedimentary Research*, *80*(9), 781–790. https://doi.org/10.2110/jsr.2010.072

Yokokawa, M., Kishi, M., Masuda, F., & Yamanaka, M. (1995). Climbing Ripples Recording the Change of Tidal Current Condition in the Middle Pleistocene Shimosa Group, Japan. In B. W. Flemming, A. Bartholom, A. Bartholomä, & B. W. Flemming (Eds.), *Special publication number 24 of the International Association of Sedimentologists. Tidal signatures in modern and ancient sediments* (pp. 301–311). Blackwell Science. https://doi.org/10.1002/9781444304138.ch20

Yokokawa, M., Masuda, F., & Endo, N. (1995). Sand Particle Movement on Migrating Combined-Flow Ripples. *Journal of Sedimentary Research*, *65A*, 40–44. https://doi.org/10.1306/D4268018-2B26-11D7-8648000102C1865D

Zavala, C. (2019). The new knowledge is written on sedimentary rocks – a comment on Shanmugam's paper "the hyperpycnite problem". *Journal of Palaeogeography*, *8*(1). https://doi.org/10.1186/s42501-019-0037-3

Zavala, C. (2020). Hyperpycnal (over density) flows and deposits. *Journal of Palaeogeography*, *9*(1), Article 17. https://doi.org/10.1186/s42501-020-00065-x

Zavala, C., & Arcuri, M. (2016). Intrabasinal and extrabasinal turbidites: Origin and distinctive characteristics. *Sedimentary Geology*, *337*, 36–54. https://doi.org/10.1016/j.sedgeo.2016.03.008

Zavala, C., Arcuri, M., Di Meglio, M., Díaz, H. G., & Contreras, C. (2011a). A Genetic Facies Tract for the Analysis of Sustained Hyperpycnal Flow Deposits. In R. M. Slatt & C. Zavala (Eds.), *Sediment Transfer from Shelf to Deep Water—Revisiting the Delivery System.* American Association of Petroleum Geologists. https://doi.org/10.1306/13271349St613438

Zavala, C., Arcuri, M., Di Meglio, M., Zorzano, A., Otharán, G., Irastorza, A., & Torresi, A. (2021). Deltas: a new classification expanding Bates's concepts. *Journal of Palaeogeography*, *10*(1), Article 23. https://doi.org/10.1186/s42501-021-00098-w

Zavala, C., Arcuri, M., & Valiente, L. B. (2011b). The importance of plant remains as diagnostic criteria for the recognition of ancient hyperpycnites. *Revue De Paleobiologie*, *11*, 457–469.

Zavala, C., Arcuri, M., Zorzano, A., Trobbiani, V., Torresi, A., & Irastorza, A. (2024). Deltas: New paradigms. *The Depositional Record*, Article dep2.266. Advance online publication. https://doi.org/10.1002/dep2.266

Zavala, C., Gamero, H., & Arcuri, M. (2006). *Lofting rhythmites: a diagnostic feature for the recognition of hyperpycnal deposits*. 2006 GSA Annual Meeting, 22–25 October, Philadelphia, PA., USA. Topical session T136: River Generated Hyperpycnal Events and Resulted Deposits in Modern and Ancient Environments.

Zavala, C., & Pan, S. (2018). Hyperpycnal flows and hyperpycnites: Origin and distinctive characteristics. *Lithologic Reservoirs*, *30*(1), 1–27.

Zhang, J., Sun, Z., Liu, L., & Li, Y. (2019). Sedimentary model of K-Successions Sandstones in H21 Area of Huizhou Depression, Pearl River Mouth Basin, South China Sea. *Open Geosciences*, *11*(1), 997–1013. https://doi.org/10.1515/geo-2019-0077

Zhang, Q., & Suhayda, J. N. (1994). Behavior of marine sediment under storm wave-loading. *Marine Georesources & Geotechnology*, *12*(3), 259–269. https://doi.org/10.1080/10641199409388266

Zheng, X., Li, A., Wan, S., Jiang, F., Kao, S. J., & Johnson, C. (2014). ITCZ and ENSO pacing on East Asian winter monsoon variation during the Holocene: Sedimentological evidence from the Okinawa Trough. *Journal of Geophysical Research: Oceans*, *119*(7), 4410–4429. https://doi.org/10.1002/2013JC009603

Ziegler, W. (1970). *Erläuterungen zu Blatt 4713 Plettenberg: 2. völlig neu bearbeitete Auflage*. Geologisches Landesamt Nordrhein-Westfalen.

Ziegler, W. (1978). *Erläuterungen zu Blatt 4813 Attendorn: 2. neu bearbeitet Auflage*. Geologisches Landesamt Nordrhein-Westfalen.